

OPEN-FILE REPORT 05-3

**Geologic Map of the South Half of the Culebra Peak Quadrangle,
Costilla and Las Animas Counties, Colorado**

**Description of Map Units, Stratigraphy, Structure,
Economic Geology, Geologic Hazards and
Engineering Constraints, and Water Resources**

By
Robert M. Kirkham¹, John W. Keller², Jason B. Price², and Neil R. Lindsay³

¹ Consulting Geologist, Alamosa, Colorado

² Colorado Geological Survey, Denver, Colorado

³ Colorado Geological Survey, Alamosa, Colorado

Bill Owens, Governor,
State of Colorado



Russell George, Executive Director,
Department of Natural Resources



Vincent Matthews,
State Geologist and Division Director,
Colorado Geological Survey

Denver, Colorado
2005

FOREWORD

The Colorado Department of Natural Resources is pleased to present the Colorado Geological Survey Open File Report 05-3, *Geologic Map of the southern half of the Culebra Peak Quadrangle, Costilla and Las Animas Counties, Colorado*. Its purpose is to describe the geologic setting of the southern half of this 7.5-minute quadrangle, the majority of which is located in Costilla County. Field work for this project was conducted during the summer of 2004 by consulting geologist Robert M. Kirkham, CGS staff geologist John W. Keller, and field assistants Jason B. Price and Neil R. Lindsay.

This mapping project was funded jointly by the U.S. Geological Survey through the STATEMAP component of the National Cooperative Geologic Mapping Program which is authorized by the National Geologic Mapping Act of 1997, Agreement No. 04HQOAG0075, and the Colorado Geological Survey using the Colorado Department of Natural Resources Severance Tax Operational Funds. The CGS matching funds come from the severance tax paid on the production of natural gas, oil, coal, and metals.

Vince Matthews
State Geologist and Division Director

CONTENTS

Foreword	ii
Introduction	1
Description of Map Units.....	3
Surficial Deposits	3
Alluvial Deposits.....	4
Mass-Wasting Deposits.....	5
Alluvial and Mass-Wasting Deposits.....	7
Glacial Deposits.....	7
Periglacial Deposits	8
Diamicton.....	9
Bedrock.....	9
Tertiary Sedimentary and Igneous Rocks	9
Mesozoic and Paleozoic Sedimentary Rocks	16
Lower Paleozoic or Neoproterozoic Rocks	19
Paleoproterozoic Intrusive Rocks	20
Paleoproterozoic Layered Rocks.....	22
Stratigraphy	23
Structure	28
Economic Geology	33
Geologic Hazards and Engineering Constraints	35
Water Resources	37
Acknowledgments	38
References Cited.....	39
Appendix 1. Whole-Rock Major-Element Geochemical Analyses.....	44
Appendix 2. Trace-Element Geochemical Analyses	45

FIGURES

1. Location map of the south half of Culebra Peak quadrangle.....	1
2. Quaternary time chart.	3
3. Total alkali-silica diagram of volcanic and selected intrusive rock samples.	12
4. View of cinder deposits (unit Tbtc) exposed in cliff.	14
5. Hoodoos on the southeast side of the Top of the World.....	15
6. Stereonets and rose diagrams of foliation planes.....	29
7. View of Split Mountain looking north-northeast.	31
8. Ricardo Creek fault is exposed in the cut slope of a new road.	32
9. Overturned clastic beds in the Madera Formation.	33
10. Photograph of headscarp of a landslide in fractured aplite and augen gneiss.....	36

TABLE

1. Argon ⁴⁰ /Argon ³⁹ ages of Tertiary igneous rocks	13
--	----

INTRODUCTION

Geologic mapping of the southern half of the Culebra Peak quadrangle was undertaken by the Colorado Geological Survey (CGS) as part of the STATEMAP component of the National Cooperative Geologic Mapping Program. This geologic map is the fourth map by the CGS in this region (fig. 1). The three previous maps include: Fort Garland SW quadrangle (Kirkham and Heimsoth, 2003); Taylor Ranch quadrangle (Kirkham and others, 2003); and La Valley quadrangle (Kirkham and others, 2004). The north half of the Culebra Peak quadrangle was not mapped, primarily because of access restrictions.

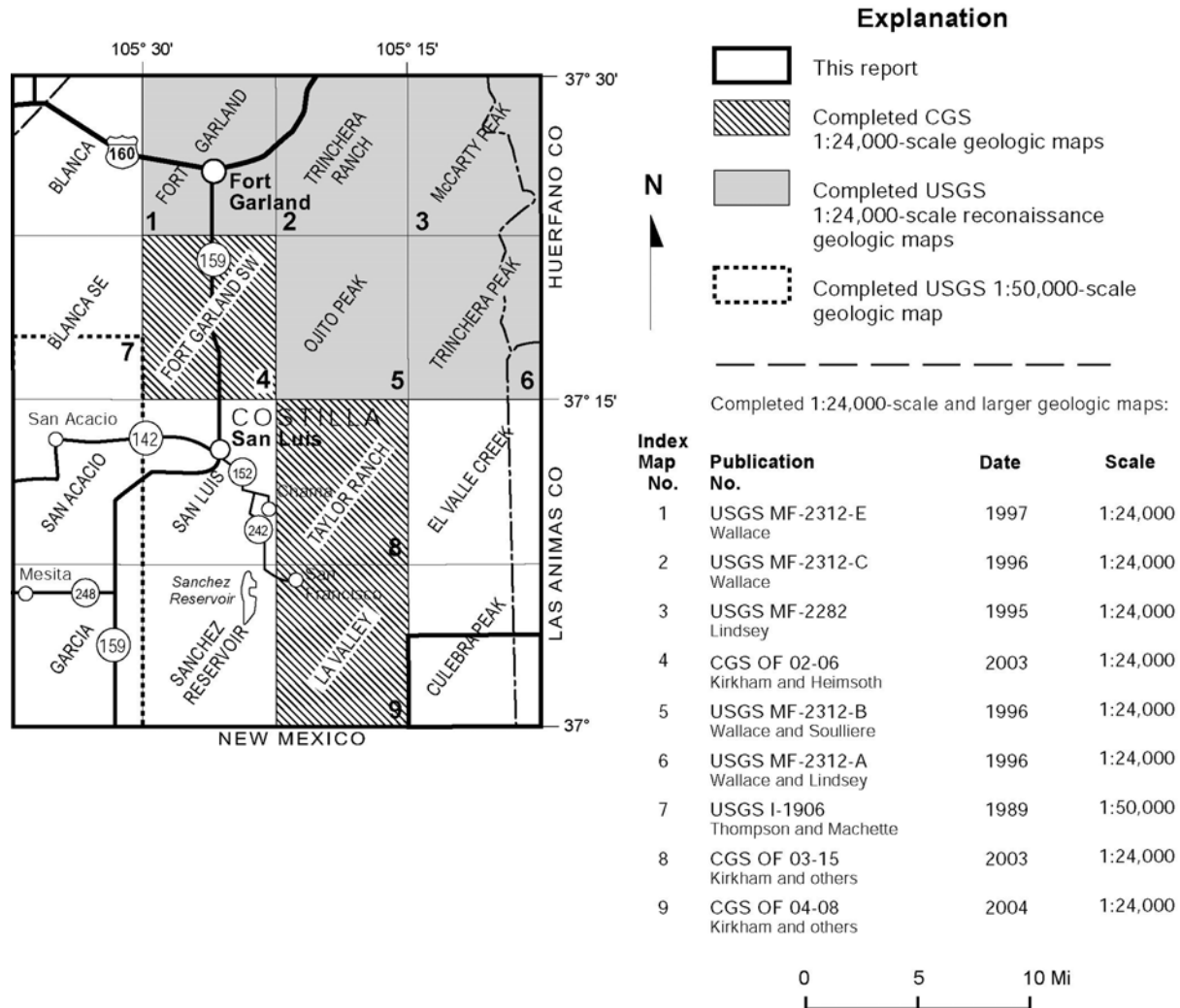


Figure 1. Location map of the south half of the Culebra Peak quadrangle, and status of geologic mapping in adjacent areas.

The map area covers parts of Costilla and Las Animas Counties and includes a low saddle in the crest of the Culebra Range and the flanking hills to east of the crest. Field work in this remote area was conducted from June through August, 2004. R.M. Kirkham and his field assistant N.R. Lindsay mapped the Phanerozoic rocks and surficial deposits. J.W. Keller and J.B.

Price mapped the Precambrian rocks. Access restrictions precluded field work in the northeast corner of the map area.

Grain-size terminology used for sedimentary deposits follows the modified Wentworth grain-size scale (Ingram, 1989). This classification system defines pebbles, cobbles, and boulders as differing sizes of gravel. These terms are commonly used by many geologists for rounded clasts deposited in fluvial and beach environments (e.g. Jackson, 1997). We herein use these terms only to describe the size of the clasts, not the genetic origin. Terms used for sediment sorting are those of Folk and Ward (1957).

Selected rock samples were analyzed for major elements (Appendix 1). The total alkali-silica plot of Le Bas and others (1986) was used to classify the analyzed volcanic rocks. Names for intrusive rocks were assigned on the basis of the quartz-alkali feldspar-plagioclase (QAP) diagram of Streckeisen (1976), aided by a homologue of the QAP diagram developed for use with whole-rock chemical analyses of igneous rocks (La Roche, 1992). Two samples of sheared or brecciated Proterozoic gneissic granite were analyzed for trace elements (Appendix 2).

Only a handful of official geographic names are shown on the base map. Since geographic names are useful when describing the geology of the map area, we adopt local names for or assign informal names to: (1) “Split Mountain”, the 12,843-ft-high mountain in the northwest part of the map area; (2) “Top of the World”, the 12,284-ft-high mountain in the west-central part of the map area; (3) “Lookout Mountain”, the 11,682-ft-high mountain in the center of the map area; (4) “Round Hill”, a 10,775-ft-high hill about one mile northeast of Lookout Mountain; and (5) “Dakota Hogback”, a northeast-trending, narrow ridge in the southeast corner of the map area. Quotation marks are not used with these informal names in the remainder of the report.

Prior published geologic maps of the area that includes the south half of the Culebra Peak quadrangle are regional and of small scale. A regional tectonic map (scale 1:1,000,000) of the Rio Grande rift by Tweto (1978) covers the map area, as do the 1:500,000-scale geologic maps of the entire state by Burbank and others (1935) and Tweto (1979) and the 1:250,000-scale geologic map of the Trinidad 1° x 2° quadrangle by Johnson (1969). Stone (1932) produced an unpublished small-scale reconnaissance map that includes part of the area mapped during this project. A 1:24,000-scale geologic map of the 7.5-minute quadrangle to the west of the map area is available (Kirkham and others, 2004), and an unpublished map of the quadrangle to the south (Pillmore, 2004) was provided by the U.S. Geological Survey.

DESCRIPTION OF MAP UNITS

SURFICIAL DEPOSITS

Surficial geologic deposits in the south half of the Culebra Peak quadrangle are subdivided into map units on the basis of either genesis or landform and also relative age. Most of the surficial deposits in the map area are not well exposed. The best exposures are in the eroded banks of streams and arroyos and in roadcuts. Because of the limited exposures, the physical attributes of these units, such as thickness, texture, stratification, and composition, are based on observations made at only a few locations, and their origin is often deduced only on the basis of geomorphic characteristics.

Surficial units more than 3 to 5 ft thick are shown on the map. Deposits associated with distinct landforms locally may be thinner than 3 ft. Surficial deposits with a mapped width of about 100 ft or less generally are too small to show on the 1:24,000-scale map. Deposits of residuum and felsenmeer are not mapped because they formed in place and have not been transported significant distances. Contacts for many surficial units were located using geomorphic characteristics, and some contacts are gradational.

Divisions of the Quaternary used herein (fig. 2) are from Widmann and others (2004), who relied upon the work of Fullerton and others (2003). Absolute ages have not been obtained for any of the surficial deposits in the map area. Characteristics such as stratigraphic relations, position in the landscape, degree of weathering, and, where exposed, pedogenic soil development were used to estimate the relative ages of the surficial deposits.

Formal time divisions		Informal time divisions	Informal nomenclature for glacial deposits	Approx. age (sidereal years)
Quaternary Period	Holocene Epoch			
	Pleistocene Epoch	late Pleistocene	— ? — ? — ? — ? — Pinedale	11,680
			— ? — ? — ? — ? —	55,000
		middle Pleistocene	— ? — ? — ? — ? — Bull Lake	128,000
		early Pleistocene	— ? — ? — ? — ? — Pre - Bull Lake	778,000
Tertiary Period (part)	Pliocene Epoch			1,806,000

Figure 2. Quaternary time chart (from Widmann and others, 2004).

Soil-horizon names used here are those of the Soil Survey Staff (1975) and Guthrie and Witty (1982), and the stages of secondary carbonate morphology are from Gile and others (1966), with the modifications of Machette (1985). Concurrent soil mapping by the U.S.

Department of Agriculture's Natural Resource Conservation Service aided our attempt to use pedogenic soil development as a tool to determine relative ages of the surficial map units.

ALLUVIAL DEPOSITS—Sediments deposited by flowing water in channels and on flood plains and fans. Sediments in the pre-Holocene units along Ricardo Creek, the East Fork of Costilla Creek, and El Fragoso Creek were deposited primarily as outwash from melting glaciers in the Culebra Range.

Qa₁ Alluvial unit one (Holocene)—Mainly poorly sorted, clast-supported, unconsolidated, sandy gravel of all sizes, gravelly sand, silty sand, and sandy silt in channels, flood plains, and low-lying terraces. Deposits in alluvial unit one range from poorly bedded to well bedded and may have cut-and-fill channels. Locally the unit includes very poorly sorted, matrix-supported gravelly silt and sand that probably were deposited by debris flows from tributary drainages. Most clasts in unit Qa₁ are subrounded to subangular; a few are rounded or angular. Many clasts are fresh and sound; weathered clasts probably were recycled from conglomerate beds in the Santa Fe Group. Deposits of unit Qa₁ usually lack any appreciable soil development or have only weakly developed soil profiles. They were deposited during oxygen isotope stage 1, perhaps during episodes of Holocene neoglaciation. Because the base of unit Qa₁ is not exposed, the thickness of this unit is unknown. It probably averages 5 to 25 ft thick, but locally could be thicker.

Qa₂ Alluvial unit two (upper Pleistocene)—Alluvial unit two consists of glacial outwash that is lithologically similar to alluvial unit one (Qa₁). Unit Qa₂ underlies terrace surfaces along El Fragoso and Ricardo creeks. It is mainly poorly sorted and clast supported. Most clasts are unweathered or very slightly weathered. Pedogenic soils formed on unit Qa₂ have moderate oxidized Bw horizons, weak clayey (argillic) Bt horizons, and calcareous Cca horizons with stage I to weak stage II carbonate morphology. Deposits of unit Qa₂ locally grade upstream to morainal deposits of unit Qm₁, which are Pinedale in age (oxygen isotope stage 2) and generally considered to be about 16 to 35 ka. Thickness of this unit is unknown.

Qa Alluvial units one and two, undivided (Holocene and upper Pleistocene)—Includes deposits of alluvial unit one and alluvial unit two in the valleys of El Fragoso, Ricardo, Little Vermejo, and Fish creeks that cannot be mapped separately at a scale of 1:24,000.

Qao Older alluvium (middle or lower? Pleistocene)—Includes a single deposit of terrace alluvium on the north side of Ricardo Creek, on the southeast side of Lookout Mountain. These sandy pebble, cobble, and boulder gravels lie about 100 to 120 ft above the creek. Their height above Ricardo Creek suggests a pre-Pinedale age. Unit Qao may have been deposited during the late middle Pleistocene (oxygen isotope stage 6) around 130 to 150 ka, or it could have been deposited during an older period of glaciation.

MASS-WASTING DEPOSITS—Deposits on hillslopes and adjacent valley floors that were transported downslope primarily by gravity and not transported within, on, or under another medium such as flowing water, ice, or wind (Jackson, 1997). Water can be an important element in mass wasting, and it commonly triggers the movement. However, water is merely a part of the moving mass, not the transporting agent. Landslide deposits, colluvium, talus, and debris flows are the principal types of mass-wasting deposits in the quadrangle. Most mass-wasting deposits are poorly sorted and unstratified. The classification system of Cruden and Varnes (1996) is used to describe the type of slope movement.

Qlsy Younger landslide deposits (Holocene)—Younger landslide deposits have fresh and distinct scarps, pressure ridges, ground cracks, hummocks, closed depressions, lateral margins, and toes. There are four younger landslide deposits in the map area. The younger landslide deposit on the northwest side of the Top of the World is a small, shallow debris slide with prominent lateral levees on its margins. This landslide initiated in colluvium and residuum that overlies dacitic flows (unit Td) between the Fall of 1988 and Fall of 1999, as the landslide is visible on aerial photography flown in 1999 but not on photography from 1988. Another small younger landslide deposit is about one-half mile south of the dissected cinder cone (unit Tbtc) on the southeast side of the Top of the World. This landslide is an earth flow or debris slide that remobilized part of an existing landslide deposit (unit Qls). Its age also is constrained by the 1988 and 1999 aerial photography.

The largest younger landslide in the map area developed in residuum and colluvium that overlies granitic augen gneiss (unit Xag) about $\frac{3}{4}$ of a mile southeast of Split Mountain. This rotational landslide looks very fresh on aerial photograph flown on August 23, 1968, therefore it probably initiated shortly prior to 1968. The small younger landslide near the southern edge of the map area and east of Devils Park involved volcanoclastic sediments (unit Tvc). This very recent debris slide formed after the 1999 aerial photographs were flown.

Qptr Protalus-rampart deposits (Holocene)—Protalus-rampart deposits consist of unsorted, unstratified, angular rock fragments that (1) fell from the cliff or steep rocky slope above a snowfield, (2) rolled, bounced, or slid down the snowfield, and (3) accumulated at the toe of the snowfield. After the snowfield melts, the protalus rampart forms an arcuate ridge that stands some distance beyond the base of the slope from which it was derived. This unit typically lacks matrix material at and near the ground surface but may have considerable silty and sandy matrix at depth. The protalus-rampart deposits post-date the late Pleistocene Pinedale glaciation. They may have been deposited during or immediately following minor glacial advances in the Holocene when large snow fields existed in the cirques. Maximum thickness is about 30 feet.

Qc Colluvium (Holocene and upper Pleistocene)—Deposits of sandy or silty, fine to coarse gravel and gravelly sand and silt that are on or at the foot of hillslopes. As used here, colluvium generally follows the definition of Hilgard (1892) in that it (1) is derived locally and transported only short distances, (2) is not distributed by channelized water flow, (3) contains clasts of varying size, (4) has little or no sedimentary structures or stratification, which are typically caused by channelized flow of water, but (5) may include minor amounts of coarsely stratified sheetwash and debris-flow deposits. Unit Qc also locally includes small landslide and talus deposits too small to map separately. Clasts in colluvium typically are angular to subangular, except in areas where the bedrock source areas for the colluvium contain well-

rounded clasts, as for example in the conglomeratic beds of the Santa Fe Group and Madera and Sangre de Cristo Formations. Maximum thickness of colluvium is estimated at 30 ft.

Qta Talus (Holocene and upper Pleistocene)—Chiefly angular rock debris deposited at the base of cliffs composed of well-indurated bedrock. The debris came from the cliffs by rockfalls, rock slides, rock topples, snow avalanches, and debris flows. Most talus consists of gravel-sized material, and boulders as large as 8 to 10 ft in diameter locally are common. Talus typically lacks matrix material, at least at or near the surface. Talus is widespread where Proterozoic rocks form the headwalls of cirques in Ricardo and El Fragoso Creeks, and where volcanic rocks crop out in cliffs along the range crest. Talus deposits adjacent to the Tertiary granodiorite in the northeast part of the map area may in part owe their origin to in-place frost wedging of subjacent bedrock rather than mass wasting. Maximum estimated thickness of talus is about 50 ft.

Qls Landslide deposits (Holocene and upper Pleistocene)—Landslide deposits are characterized by hummocky topography and lobate form and include debris slides and rotational, translational, and complex landslides. Uphill advancing, retrogressive landslides are abundant along the range crest where competent volcanic flows overlie very weakly lithified Santa Fe Group sedimentary deposits. Several rotational and translational landslides formed in morainal deposits, solifluction deposits, and even in Proterozoic granitic augen gneiss, perhaps in areas where fracturing is prevalent. Landslides are rare in other Proterozoic units and in the Paleozoic rocks, but they are widespread in areas underlain by the shale-rich Upper Cretaceous rocks (unit Ku) in the southeast corner of the map area.

Large blocks of rotated but relatively intact blocks of bedrock are locally found in landslide deposits. These blocks of bedrock, some of which are toreva blocks, are present in the upper reaches of Ricardo Creek and in the East Fork Costilla Creek. Bedrock blocks in the landslides of upper Ricardo Creek consist of Proterozoic crystalline rock. Volcanic flows compose the blocks of bedrock in the retrogressive landslides of the East Fork Costilla Creek; further advancement uphill will eventually destroy the volcanic caprock of the range crest. Landslide deposits locally exceed 100 ft in thickness, but most are typically 10 to 30 ft thick.

Qlso Older landslide deposits (Pleistocene)—Older landslide deposits have subdued morphologic features or have been dissected by erosion, suggesting the deposits are middle Pleistocene or older. Older landslide deposits are preserved in the southwest part of the map area. They formed in response to retrogressive failure of upland surfaces that have a caprock of indurated volcanic flows and underlying weakly lithified late Tertiary sedimentary deposits. As the slope movements retrogressed and advanced farther into the caprock, the initial landslide deposits at the base of the landslide complex became inactive. Maximum thickness of the older landslide deposits locally may exceed 120 ft.

ALLUVIAL AND MASS-WASTING DEPOSITS—Alluvial and mass-wasting deposits are mapped as a single unit when they are juxtaposed and are too small to show individually, or where the contacts between them are not clearly defined. Fan deposits also are classified as mixed alluvial and mass-wasting deposits because in addition to alluvium they include significant volumes of sediment from debris flows, which are generally considered to be a form of mass wasting (e.g. Cruden and Varnes, 1996; Hungr and others, 2001).

Qfy Younger fan deposits (Holocene and upper Pleistocene)—Includes sediment in small, geomorphically distinct fans at the mouths of tributary valleys and large, coalesced fan complexes along the larger valleys. Younger fan deposits are chiefly very poorly sorted to moderately well-sorted, clast-supported, alluvial sandy gravel, gravelly sand, and sand. Locally they include matrix-supported debris-flow deposits that generally are composed of matrix-supported gravel, sand, and silt. Some of the beds are stratified. Clasts contained in younger fan deposits are mainly subangular to subrounded. Maximum thickness of the younger fan deposits is estimated at 40 ft, but commonly the deposits are thinner.

Qac Alluvium and colluvium, undivided (Holocene and upper Pleistocene)—Unit Qac consists of sediment deposited in (1) channels, flood plains, and low terraces in tributary drainages, and (2) colluvium and sheetwash along valley margins and sidehills. The alluvial component of the unit is very poorly sorted to well sorted and ranges from sandy pebble, cobble, and boulder gravel to stratified fine sand and silt. Clasts in the alluvial component are angular to subrounded. The colluvial component consists of very poorly sorted, unstratified or poorly stratified, gravelly to silty sand, sandy to silty gravel and gravelly sandy silt. Clasts in the colluvial component are chiefly angular to subangular. Thickness of unit Qac is estimated to range from 3 to 25 ft thick.

Qfo Older fan deposits (Pleistocene)—Older fan deposits underlie an inactive fan surface in the valley of El Fragoso Creek, near the west edge of the map area. The stream that deposited the older fan sediments has now incised 20 to 60 ft into the sediments. Estimated maximum thickness of unit Qfo is about 40 ft.

Qaco Older alluvium and colluvium, undivided (Pleistocene)—Unit Qaco includes remnants of alluvium and colluvium that underlie terrace surfaces and drainage divides along Fish, Ricardo, and Little Vermejo Creeks. Physical characteristics of this unit are similar to those of unit Qac. Thickness of unit Qaco locally may exceed 20 ft, but commonly it is much thinner.

GLACIAL DEPOSITS—Sediment deposited by, or adjacent to, glacial ice and preserved in morainal landforms. Most of the glacial deposits in the map area consist of till, which is the term for nonsorted, nonstratified sediment directly deposited by ice without reworking by meltwater. Stratified sediment and mass-wasting deposits, however, are locally present, primarily in end and terminal moraines. Because till is not the only type of sediment in the moraines, we herein refer to the surficial deposits beneath these landforms as morainal deposits. The lower limit of glacial deposits is at an elevation of about 9,800 ft in the map area.

Qm1 Morainal deposit one (upper Pleistocene)—Heterogeneous deposits of mostly nonsorted, nonstratified, boulders, cobbles, and pebbles in a sand or silty sand matrix that were

deposited in lateral, terminal, end, recessional, and ground moraines. Unit Qm₁ underlies large parts of the valleys of El Fragoso and Ricardo Creeks and their tributaries. Glaciers spilled over the low divide between Ricardo Creek and a tributary to Little Vermejo Creek at the northern end of Lookout Mountain and extended down the tributary, depositing unit Qm₁ nearly to Round Hill. Unit Qm₁ also underlies a very small area in the southwest corner of the map area; these sediments were deposited by a glacier that formed in the West Fork of Costilla Creek in the adjacent La Valley quadrangle (Kirkham and others, 2004).

Fine-grained matrix locally comprises more than 50 percent of unit Qm₁. Clasts contained within unit Qm₁ are subangular to subrounded. Boulders with only minor pitting are present on the surface of the moraines underlain by unit Qm₁, and clasts in the unit are unweathered to slightly weathered. The crests of unit Qm₁ moraines are fairly sharp. Morainal deposit one is tentatively correlated with deposits of the Pinedale glaciation, which occurred during the late Pleistocene during oxygen isotope stage 2. In the upper reaches of the Ricardo Creek drainage and in the headwaters of the glaciated valley on the southeast side of the Top of the World, unit Qm₁ may include sediment deposited or remobilized during a neoglacial ice advance in the Holocene. Unit Qm₁ probably exceeds a thickness of 100 ft in some areas, but elsewhere it typically is 10 to 40 ft thick.

Unit Qm₁ is locally subdivided into younger (unit Qm_{1y}) and older (unit Qm_{1o}) deposits, chiefly on the basis of soil development and the surface morphology of the moraines. Unit Qm_{1y} may have been deposited late during the Pinedale glaciation, while unit Qm_{1o} may be an early Pinedale deposit. Morainal deposits in the cirques of Ricardo Creek and its tributaries and the sediment beneath the two moraine crests southeast of the Top of the World may be neoglacial deposits.

Qm₂ Morainal deposit two (upper middle Pleistocene)—Sediment in unit Qm₂ is similar to the sediment in unit Qm₁. Remnants of unit Qm₂ are preserved in El Fragoso Creek and in the tributary to Ricardo Creek on the southeast side of the Top of the World. The moraine crests of unit Qm₂ are more rounded and subdued than the moraine crests of unit Qm₁, and the boulders exposed on the surface of unit Qm₂ are fewer in number and more weathered than those on the surface of unit Qm₁. Unit Qm₂ is tentatively correlated with the Bull Lake glaciation, which is late middle Pleistocene in age (oxygen isotope stage 6), but it could also have been deposited during oxygen isotope stage 4. Morainal deposit Qm₂ has an estimated maximum thickness of about 120 ft.

PERIGLACIAL DEPOSITS—Deposits formed in cold environments by freeze-thaw action, solifluction, and nivation.

Qs Solifluction deposits (Holocene and upper Pleistocene)—Angular to subrounded pebbles, cobbles, and large boulders in a chiefly sandy matrix. Solifluction deposits were deposited in the more poorly drained parts of alpine and subalpine areas as a result of the slow, viscous, downslope flowage of water-saturated surficial deposits over frozen ground. Frost action, augmented by meltwater from alternate freezing and thawing of snow and ice, often initiates the movement. Areas mapped as solifluction deposits are characterized by hummocky terrain, linear swales and ridges, and numerous seeps and springs. Minor ground cracks and fissures also may be present. Lobes and terracettes with small ledges or benches that can be

several feet high are common landforms associated with solifluction deposits. Solifluction deposits are estimated to be about 3 to 15 ft thick.

DIAMICTON—Flint and others (1960) proposed the nongenetic term “diamicton” for nonlithified, poorly sorted, terrigenous sediment containing a wide range of particle sizes. It is used herein for till-like deposits of uncertain origin in and east of Devils Park, which is in the south-central part of the map area.

Qdi Diamicton (upper Pleistocene)—Subangular to subrounded cobbles, pebbles, and boulders with a sand or silty sand matrix. Matrix may comprise as much as 50 percent of the sediment. Most boulders are 1 to 3 ft in diameter, but some are as long as about 7 ft. A sudden major landslide may have created these deposits, but they could also be till, chiefly because subdued moraine-like landforms are locally present. Refer to the Stratigraphy section for a discussion on the origin of the diamicton. Soils formed on diamicton are similar to soils on till and outwash correlated with deposits of the Pinedale glaciation. Boulders with only minor weathering are locally abundant on the ground surface of diamicton. Diamicton may attain a thickness of about 100 ft but generally is 10 to 40 ft thick.

Qdio Older Diamicton (upper middle Pleistocene)—Older diamicton, which is found in a single area northeast of Devils Park, is lithologically similar to diamicton in unit Qdi. The unit is well exposed in a road cut along Ricardo Creek. Pedogenic soils exposed in this road cut are similar to the soils observed in the upper middle Pleistocene morainal deposits of unit Qm2. Boulders are less numerous, smaller in diameter, and more weathered on the ground surface of older diamicton than unit Qdi. Maximum thickness of older diamicton is estimated at 40 ft.

BEDROCK

TERTIARY SEDIMENTARY AND IGNEOUS ROCKS

Santa Fe Group (upper Oligocene? and Miocene)

The Santa Fe Group consists of a thick sequence of sedimentary strata and intercalated volcanic flows that were deposited within the Rio Grande rift. Only the sedimentary deposits and volcanic rocks in the middle and lower parts of the Santa Fe Group crop out within the map area. The Santa Fe Group is subdivided in the map area into one informal sedimentary member and four informal volcanic members.

Informal sedimentary member of the Santa Fe Group

Tsfl Lower Santa Fe Group sedimentary rocks (late Oligocene? and Miocene)—Unit Tsfl includes the widespread rift-related sedimentary deposits that either underlie or

are intercalated with the middle Miocene volcanic flows of unit Tbt. The lower Santa Fe sedimentary deposits are very poorly exposed in the map area. A single good exposure of these rocks was found in a cut slope along the jeep trail to Leandro Lake. Here, the rocks are weakly lithified and consist of sandy cobble and pebble conglomerate with sparse boulders, conglomeratic sandstone, fine- to coarse-grained sandstone, and sandy silt that was deposited in fluvial environments. Clasts are subangular to subrounded and composed mostly of gneissic granite, granitic augen gneiss, red-brown arkosic sandstone, conglomeratic sandstone, and conglomerate, with minor amounts of mafic volcanic rocks. Elsewhere in the map area, lower Santa Fe sediments form small, sparse, poor exposures.

Basal strata in the lower Santa Fe sedimentary member are best exposed in the northwest part of the map area. The basal strata are rich in clasts derived from Paleozoic redbed sedimentary bedrock. Proterozoic and volcanic lithologies comprise a greater percentage of the clasts in overlying beds. In Devils Park relatively thin volcanic flows of unit Tbt are intercalated with the lower Santa Fe sediments.

On the northwest side of the Top of the World, the apparent thickness of the lower Santa Fe Group sediments that underlie the volcanic flows of unit Tbt is about 800 ft. To the south, in and west of Devils Park, these sediments may be as much as 2000 ft thick. These thickness estimates of the lower Santa Fe sedimentary member are similar to those reported by Kirkham and others (2004) west of the map area.

The age of the lower Santa Fe Group sedimentary rocks is primarily constrained by the ages of volcanic flows that overlie or are intercalated with it. To the west and southwest of the map area, flows that directly overlie the thick, main body of lower Santa Fe sediments have been dated at 14.80 ± 0.09 Ma (Kirkham and others, 2004) and 15.16 ± 0.03 Ma (Miggins, 2002; Miggins and others, 2002) for unit Tsfl. A volcanic flow intercalated with lower Santa Fe sediments in Devils Park (sample CP106) yielded an age of 12.02 ± 0.07 Ma (Esser, 2005).

Informal volcanic members of the Santa Fe Group

Tdb Dacitic breccia (Miocene)—A single small outcrop of dacitic breccia occurs on the east-southeast side of the Top of the World. The breccia consists of a massive deposit of angular cobbles, pebbles, and boulders in a chiefly ash matrix. Although bedding was very difficult to discern, the deposit appears to roughly parallel the slope on which it lies. In hand specimen, the light-gray breccia clasts are similar to the dacitic flows of unit Td. A thin section cut from one of the breccia clasts was about 70 percent plagioclase-rich groundmass and about 25 percent plagioclase phenocrysts, with a few percent of hornblende and biotite phenocrysts and minor augite phenocrysts. The breccia clast from unit Tdb (sample CP271) contains 1 to 2 percent more silica and about 0.5 percent less total alkali than the four analyzed samples of dacite from unit Td (Appendix 1). On figure 3, the breccia clast plots in the dacite field near the unit Td samples, which are in the trachydacite field. Similarities in the petrology and chemistry of units Td and Tdb, along with their spatial relationships, suggest the dacitic flow breccia of unit Tdb was emplaced on the flank of a dacitic lava dome at the Top of the World.

Td Dacite (Miocene)—Light-gray to light-pinkish-gray dacitic flows cap the crest of the Culebra Range at the Top of the World, whose shape is reminiscent of a partially eroded silicic lava dome. A plagioclase-rich matrix comprises about 60 to 70 percent of the dacitic rocks. Phenocrysts, which make up the remainder of the rock, are mostly plagioclase, with lesser amounts of hornblende (up to 6 mm long) and minor biotite and augite. Four samples of dacite were chemically analyzed (Appendix 1). All four samples plot in a tight cluster in the trachydacite field near the margin of the dacite field (fig. 3), and all four are subalkaline and calc-alkaline. One sample of dacite (CP504A) was dated using $^{40}\text{Ar}/^{39}\text{Ar}$ methods during this study (Table 1). The groundmass of this sample yielded an integrated or total gas age of 12.2 ± 0.1 Ma (Esser, 2005). Miggins (2002) reported an $^{40}\text{Ar}/^{39}\text{Ar}$ age of 12.08 ± 0.6 Ma on a sample collected from the west shoulder of the Top of the World that probably was from unit Td. The dacitic flows are as much as 280 ft thick.

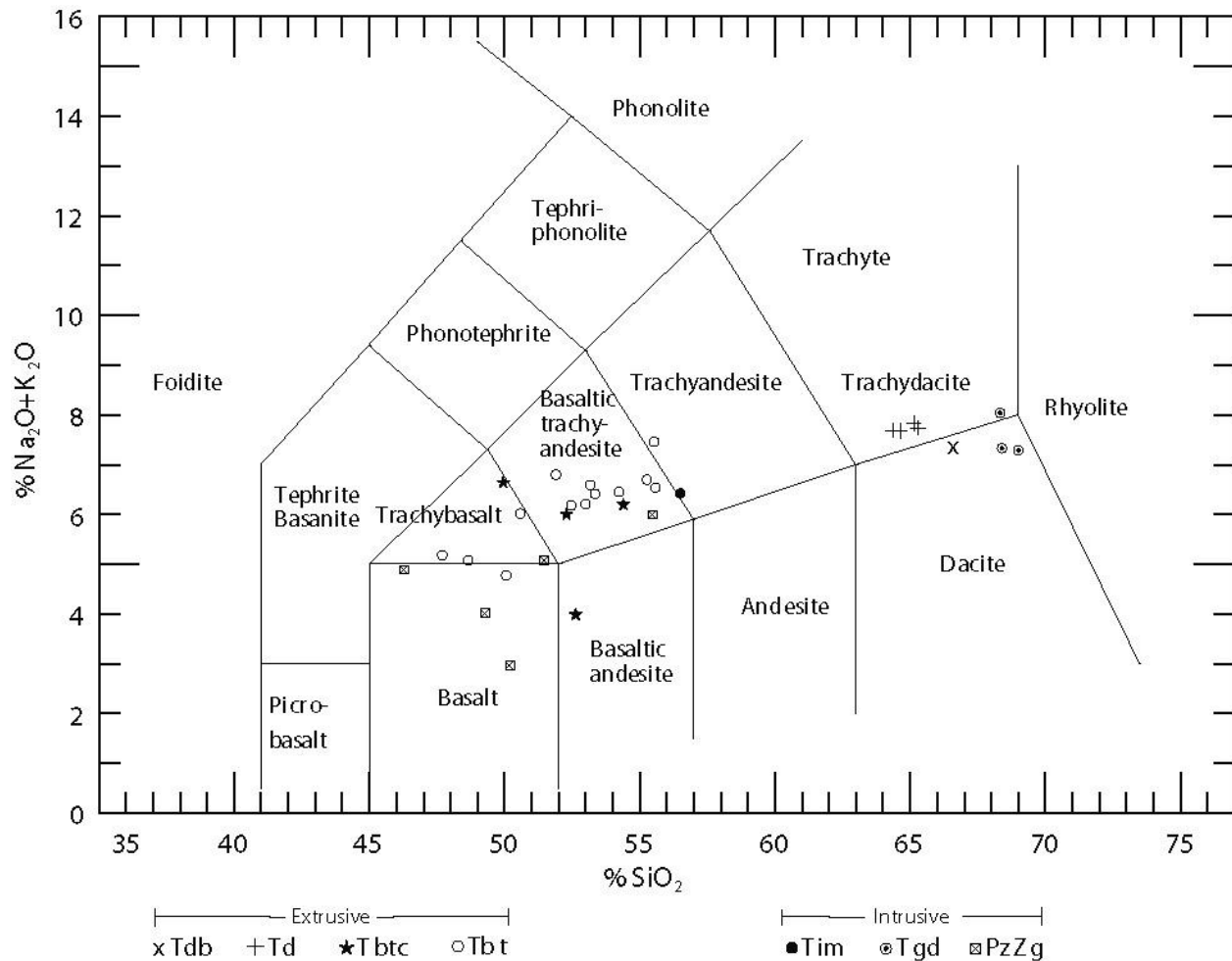


Figure 3. Total alkali-silica diagram of volcanic and selected intrusive rock samples from the south half of Culebra Peak quadrangle. Names for the volcanic rocks were assigned using this diagram. The analyses of intrusive rocks are included to allow for comparisons with the chemistry of the volcanic rocks. Classification scheme is that of Le Bas and others (1986). Values are in weight percent. See Appendix 1 for the geochemical analyses.

Tbtc Basaltic to trachybasaltic andesite cinder deposits (Miocene)—A partially dissected cinder cone is well exposed on the south and north sides of the Top of the World (fig. 4). The cone consists chiefly of 5- to 50-ft-thick beds of scoriaceous cinders in an ashy matrix and minor, lenticular, 3- to 15-ft-thick lava flows. The cinder beds are weakly to moderately welded or agglutinated, they contain volcanic bombs, and locally they erode into hoodoo landforms (fig. 5). Interlayered flows are light to medium gray and contain 2 to 3 percent large phenocrysts of clinopyroxene, sparse altered phenocrysts of olivine, and 2 to 3 percent opaque minerals in a matrix of mostly plagioclase. Samples of a flow (CP271A), bomb (CP604), flow fragment in a cinder bed (JP245), and cinders with minor matrix attached to it (JK288) were analyzed for major elements (Appendix 1). These samples plot in the basaltic trachyandesite, trachybasalt, and basaltic andesite fields of figure 3, in the general vicinity of the samples of unit Tbt. The cinder deposits on the southeast side of the Top the World have a preserved thickness of about 600 ft. The configuration of the

preserved cinder deposits suggests either the highest part of the original cinder cone was to the east, or the cinder deposits are tectonically tilted. A prominent onlap relationship or angular unconformity separates the cinder cone from overlying dacitic flows of unit Td. Miggins (2002) and Miggins and others (2002) first reported the cinder cone, and they obtained three $^{40}\text{Ar}/^{39}\text{Ar}$ ages from it that range from 11.80 ± 0.06 Ma to 11.95 ± 0.04 Ma (Table 1).

Table 1. Argon⁴⁰/Argon³⁹ ages of Tertiary igneous rocks in and adjacent to the south half of the Culebra Peak quadrangle.

Unit	Samples dated during this project (Esser, 2005) ¹	Previously reported dates	
		Miggins (2002); Miggins and others (2002) ²	Kirkham and others (2004) ¹
Td	12.2 ± 0.1 Ma (sample CP504A)	12.08 ± 0.06 Ma	
Tbtc		11.80 ± 0.06 Ma 11.87 ± 0.03 Ma 11.95 ± 0.04 Ma	
Tbt	12.02 ± 0.07 Ma (sample CP106)	10.74 ± 0.10 Ma 11.98 ± 0.10 Ma 14.22 ± 0.03 Ma 14.53 ± 0.02 Ma 15.08 ± 0.06 Ma 15.11 ± 0.03 Ma	10.80 ± 0.06 Ma 11.99 ± 0.10 Ma 14.80 ± 0.09 Ma
Tgd	minimum age 15.23 ± 0.05 Ma (sample CP46)		
Tvc		29.52 ± 0.08 Ma 31.07 ± 0.05 Ma	

¹ used an age of 27.84 Ma for Fish Canyon Tuff for calibration

² used an age of 27.55 Ma for Fish Canyon Tuff for calibration

Tbt Basaltic to trachyandesitic rocks (Miocene)—Light- to dark-gray basaltic and trachyandesitic flows, flow breccias, and minor agglutinate comprise unit Tbt. These rocks locally cap the crest of the Culebra Range and also underlie the dacitic rocks (unit Td) at the Top of the World. Unit Tbt rocks also form low ridges in Devils Park that are as much as 1600 ft lower in elevation than those on the range crest. Flows within unit Tbt commonly contain abundant phenocrysts of augite, varying amounts of phenocrystic olivine, hornblende, plagioclase, and opaque minerals, and sparse biotite. Augite is the predominant pyroxene phenocryst. Olivine phenocrysts, which are present in the more mafic flows, are slightly to strongly altered to iron oxide or iddingsite. The groundmass of flows in unit Tbt is mostly plagioclase, pyroxene, and opaque minerals. Unit Tbt flows range in thickness from about 200 to 500 ft thick.

Twelve whole-rock samples from flows in unit Tbt were chemically analyzed (Appendix 1). They plot in or very near the basaltic trachyandesite and trachybasalt fields of figure 3, and all are alkaline. The chemistry of unit Tbt flows in the map area is similar

to the chemistry of flows in unit Tbt to the west in the La Valley quadrangle (Kirkham and others, 2004). Miggins (2002), Miggins and others (2002), and Kirkham and others (2004) reported nine $^{40}\text{Ar}/^{39}\text{Ar}$ ages for samples of unit Tbt in or adjacent to the map area. These dates ranged from 10.74 ± 0.10 Ma to 15.16 ± 0.03 Ma (Table 1). One sample collected from unit Tbt in Devils Park (sample CP106) was dated during this project using $^{40}\text{Ar}/^{39}\text{Ar}$ methods. It yielded a weighted mean age of 12.02 ± 0.07 Ma (Esser, 2005).



Figure 4. View of cinder deposits (unit Tbt_c) exposed in cliff southeast of the Top of the World. The cinder deposits form the nearly continuous cliff in the upper part of the exposure. Volcanic flows of unit Tbt crop out in the smaller cliff below and to the left of the grassy slope that underlies the exposed cinder deposits.



Figure 5. Hoodoos on the southeast side of the Top of the World are composed mostly of cinder beds (unit Tbtc). The beds dip to the right, suggesting the original eruptive center was to the left or that the beds are tectonically tilted. Large clast at the top of the closest hoodoo is about 4 ft thick. The grassy meadows in the distance to the left of the closest hoodoo are within Devils Park.

Tgd Granodiorite (Miocene)—A granodiorite stock and an associated suite of sills (unit Tgd) intruded the Upper Pennsylvanian Sangre de Cristo Formation in the northeast part of the map area. Most of the stock and sills are variably altered light-gray porphyry. An aphanitic groundmass of plagioclase and possibly minor amounts of hornblende comprises about 65 percent of the rock. About 30 percent of the rock is plagioclase phenocrysts, about 3 percent is hornblende and biotite phenocrysts, and opaque minerals constitute about 1 percent. At least one sill and parts of the margin of the stock consist of dark-gray vitrophyre that is about 70 percent glassy matrix, 20 percent plagioclase phenocrysts, 8 percent hornblende phenocrysts, 1 to 2 percent opaque minerals, and less than 1 percent biotite. Maximum length of the phenocrysts is about 3 mm. The vitrophyre phase suggests the magma cooled quickly at shallow depths.

Three samples of Tertiary granodiorite were geochemically analyzed; two from the stock (CP46 and CP249) and one from a dike exposed in a road cut (CP37A). All three plot in the granodiorite field of Streckeisen (1976). The Tertiary granodiorite contains 2 to 3 percent more total alkali than the dacitic rocks in the map area (units Td and Tdb; fig. 2), but has total alkali and silica contents that are similar to rhyodacite (dikes?) that crop out in the Taylor Ranch quadrangle about nine miles northwest of the granodiorite stock (Kirkham and others, 2003).

Biotite and hornblende from sample CP46 were analyzed using $^{40}\text{Ar}/^{39}\text{Ar}$ techniques (Esser, 2005). The age spectrum of the hornblende was severely disturbed and was deemed

unreliable. The age spectrum of the biotite was slightly less disturbed than the age spectrum of the hornblende, but still had high ^{40}Ar loss. A minimum age of 15.23 ± 0.05 Ma was obtained on the biotite. The intrusive probably was emplaced during the Miocene; however, it may be older.

Tim Mafic dike (Miocene or Oligocene)—A single medium-greenish-brown mafic dike appears to intrude the volcanoclastic deposits of unit Tvc near the south edge of the map area about 300 ft west of the Ricardo Creek fault. The west side of the dike abuts or is concealed by Quaternary diamicton, and the contact with volcanoclastic sediments on the east side of the intrusive body is poorly exposed. However, the igneous body of unit Tim has a different orientation than the adjacent volcanoclastic rocks, and it has finer-grained, chilled margins, which leads us to conclude it is a dike. The relatively high phenocrystic content of the rock (~35 percent) also supports an intrusive origin. Most phenocrysts are plagioclase, many of which are zoned. About 4 to 6 percent of the entire rock consists of phenocrysts of clinopyroxene, hornblende, and opaque minerals that occur in subequal proportions. Plagioclase phenocrysts are as long as 8 mm, and the hornblende phenocrysts are up to 5 mm long. A hornblende- and plagioclase-rich matrix composes about 65 percent of the rock. One sample from the mafic dike (CP29) was geochemically analyzed (Appendix 1). It plots in the quartz monzodiorite/quartz monzogabbro field of Streckeisen (1976). The sample is slightly more silicic than the Miocene volcanic rocks in unit Tbt within the map area (Appendix 1; fig. 3), but it is similar in composition to some of the Miocene volcanic flows in unit Tbt to the west in the La Valley quadrangle (Kirkham and others, 2004). An Oligocene or Miocene age is assigned to the dike, chiefly because the dike cuts Oligocene volcanoclastic sediments.

Tvc Volcanoclastic deposits (Oligocene)—Volcanoclastic sediments crop out in a few roadcuts east of Devils Park and south and west of Ricardo Creek. These weakly lithified deposits range from sandy cobble gravel to slightly pebbly and sandy silt. A gravel bed in the westernmost outcrop of volcanoclastic deposits is cemented with opal. Nearly all clasts in unit Tvc are subrounded and rounded, and they consist of volcanic flows and tuffs with heterogeneous lithologies that range from mafic to silicic in composition. The mixed clast lithologies and clast rounding indicate the clasts were eroded from a distant volcanic area and transported significant distances in a fluvial environment. Miggins (2002) and Miggins and others (2002) reported two $^{40}\text{Ar}/^{39}\text{Ar}$ ages (29.53 ± 0.08 Ma and 31.07 ± 0.05 Ma) on clasts from correlative volcanoclastic deposits to the south in The Wall quadrangle.

MESOZOIC AND PALEOZOIC SEDIMENTARY ROCKS

Ku Upper Cretaceous rocks, undivided—A thick sequence of conformable Upper Cretaceous formations comprises the bedrock on the east side of the Dakota Hogback in the southeast corner of the map area. These rocks are very poorly exposed because they are mantled by a thin veneer of surficial debris shed from the Dakota Sandstone and Purgatoire Formation and by landslide deposits. The following lithologic descriptions are from nearby areas where the Upper Cretaceous strata are better exposed, including Vermejo Park (Pillmore and Eicher, 1976) and the Cuchara quadrangle (Lindsey, 1995). In descending order, the Upper Cretaceous strata include (1) the Pierre Shale, a medium- to dark-gray shale over 2,000 ft thick; (2) gray bentonitic shale and fossiliferous limestone in the Niobrara Formation, which is about 500 to 600 ft thick; (3) dark-gray shale, calcareous shale, black fossiliferous limestone, and minor sandstone in the

approximately 250-ft-thick Carlile Shale; (4) about 130 ft of shaly limestone, calcareous shale, and bentonite in the Greenhorn Formation; and (5) the Graneros Shale, which includes about 110 ft of mostly medium-gray to black shale and silty shale and minor, thin limestone beds.

Kdp Dakota Sandstone and Purgatoire Formation, undivided (Lower Cretaceous)—The Dakota Sandstone and Purgatoire Formation form the crest or eastern flank of the Dakota Hogback in the southeast part of the map area. They disconformably overlie the Morrison Formation. Fine-grained, brown to light-gray beds of sandstone comprise the Dakota Sandstone. Crossbedding is prominent in these well-sorted, quartzose sandstones. Johnson and Stephens (1954) described thin interbeds of black carbonaceous shales in the Dakota, but these strata were not seen in the incomplete exposures of the formation that exist in the map area. The 30- to 60-ft-thick Dakota Sandstone disconformably overlies the Purgatoire Formation.

Waage (1953) divided the Purgatoire Formation in the Raton Basin into two members: an upper Glencairn Shale Member (upper shale unit of Johnson and Stephens, 1954) and a lower Lytle Sandstone Member (lower sandstone member of Johnson and Stephens, 1954). The Glencairn Shale Member consists of about 25 ft of poorly exposed dark-gray to black shale. The Lytle Sandstone Member is light-gray to light-brown, crossbedded sandstone and conglomeratic sandstone with granules and pebbles of frosted quartz grains and gray, brown, and tan chert. Limonite staining is locally prevalent along fractures and in the matrix. Most cliffy outcrops along the Dakota Hogback are held up by the tan- and brown-weathering sandstones and conglomerates in the Lytle, which is about 120 to 180 ft thick. Kues and Lucas (1987) raised the rank of the Glencairn Shale and Lytle Sandstone Members to formation status and described the disconformity between them as the most significant time break in the Lower Cretaceous section.

Jme Morrison Formation (Upper Jurassic) and Entrada Sandstone (Middle Jurassic), undivided—This unit includes the Morrison Formation and underlying Entrada Sandstone, both of which are very poorly exposed in the map area. These rocks crop out in the southeast corner of the map area on or west of the crest of the Dakota Hogback. To the north in the Cucharas Pass quadrangle, Lindsey (1996) described the Morrison Formation as about 260 ft of variegated and locally bentonitic mudstone; interbedded brown and black mudstone and gray-brown sandstone; and interbedded sandstone, gray limestone, red cherty limestone, and gypsum. Tiny windows of exposure and float suggest the Morrison strata within the map area probably are similar to the rocks described by Lindsey (1996).

The Entrada Sandstone consists of light-gray, buff, and white massive to thin-bedded sandstone. It is fine to medium grained, about 30 to 40 ft thick, and was deposited in eolian environments. The best exposure of the Entrada Sandstone is in an exploration pit about one-half mile east of the map area. The pit was excavated to evaluate the feasibility of using the Entrada to surface dirt roads. A disconformity separates the Entrada from the underlying Triassic strata.

Tjt Johnson Gap Formation and Trujillo Formation, undivided (Triassic)—Triassic rocks are very poorly exposed in the map area. Sparse, thin (<1 ft thick) ledges of Triassic-age intraformational conglomerate comprise the only outcrops within the map area. These exposed beds are greenish-gray limestone-pebble and siltstone-pebble conglomerates. A thin section cut from one of these conglomeratic beds contained rounded micritic limestone pebbles in a matrix of subrounded quartz grains cemented by calcite; this sample is classified as a peloidal

packstone. Excellent exposures of the Triassic strata, which disconformably overlie the Sangre de Cristo Formation, are found to the northeast of the map area along Johnson Creek and to the south along Ricardo Creek. Refer to the Stratigraphy section for descriptions of those nearby outcrops.

PIPsc Sangre de Cristo Formation (Lower Permian and Upper Pennsylvanian)—Reddish-brown, nonmarine, arkosic sandstone, conglomerate, conglomeratic sandstone, siltstone, and shale comprise the Sangre de Cristo Formation. These beds are stacked in fining-upward alluvial sequences that sometimes have channeled bases. Sandstone and conglomeratic beds commonly are crossbedded. Siltstone and shale beds contain ripple marks, mudcracks, cross-laminations, and small burrows. Local bleaching or reduction of the iron oxide minerals results in light-gray to light-brown colors. The conglomeratic clasts are subangular to subrounded and are composed chiefly of quartz, feldspar, and granitic and metamorphic lithologies. Thin limestone beds are present in the Sangre de Cristo Formation in nearby areas (Bolyard, 1959; Baltz, 1965; Lindsey, 1995; Wallace and Lindsey, 1996), but none were observed in the map area. Although the uppermost few feet of strata at the top of the Sangre de Cristo Formation are not exposed in the map area, they likely are similar to the pedogenically altered, yellow, green, purple, and red mottled strata that Lucas and others (1990) described to the south along Ricardo Creek.

Erosionally resistant beds in the Sangre de Cristo Formation form excellent outcrops in the drainages of Fish Creek and Little Vermejo Creek. Roadcuts provide the best exposures of these rocks in the northeastern part of the map area. Most Sangre de Cristo strata consistently strike northeast and dip 30-50° southeast. Exceptions occur where these rocks are adjacent to the Little Vermejo Creek and Ricardo Creek faults, where the rocks dip steeply east or are overturned and dip west. Basal strata of the Sangre de Cristo Formation are cut out by the Little Vermejo Creek and Ricardo Creek faults. These faults cut out more of the basal strata in the southern part of the map area than in the northern part. The preserved thickness of the Sangre de Cristo Formation within the map area is about 12,000 ft. To the north in Trinchera Peak quadrangle, where the formation conformably overlies the Madera Formation, it exceeds 13,100 ft in thickness (Wallace and Lindsey, 1996).

IPm Madera(?) Formation (Middle Pennsylvanian)—This unit consists of interbedded, gray and red-brown arkosic sandstone, conglomeratic sandstone, and siltstone, red-brown and light- to medium-gray shale, and minor dark-gray, fossiliferous limestone. These strata are tentatively correlated with the Madera Formation, but it is possible that they are part of the lower Sangre de Cristo Formation (C.J. Fridrich, 2005, written commun.).

The sandstone and conglomeratic sandstone beds are frequently crossbedded and ripple marked, and sometimes they form prominent outcrops, like those on the walls of the water gap cut by Little Vermejo Creek. Conglomerate clasts are chiefly granule to very small pebble sizes, but range up to very coarse pebble sizes. Most clasts are subrounded and composed of quartz and feldspar. Limestone beds are sparse in this unit. The only exposures of the Madera limestones are on the east side of Little Vermejo Creek in roadcuts along the new road east of Round Mountain. Algal or stromatolitic structures are locally present in the limestones, as are locally abundant marine invertebrate fossils such as bryozoans, horn corals, and brachiopods.

Madera strata crop out in two blocks in the eastern half of the map area; both blocks are bounded by thrust faults, therefore neither the top nor bottom of the formation is present. The larger block extends from the north edge of the map area southward nearly to Ricardo Creek,

where it pinches out as the bounding thrust faults converge. Excellent exposures of the Madera Formation are found in roadcuts along a recently constructed access road; good natural outcrops are present on the crest of the linear ridge that runs northward from the water gap along Little Vermejo Creek and along the steep hillslopes of the water gap. The northern end of the second fault-bounded block of Madera strata is on the western side of Ricardo Creek near the south edge of the map area. These rocks are moderately well exposed in the cut slope of a recently built road.

Brill (1952) included the Middle Pennsylvanian strata in the Madera Formation, but subsequent workers (e.g. Johnson, 1969; Vine, 1974) correlated these strata with the Minturn Formation of central Colorado. However, Lindsey (1995) retained Brill's Madera nomenclature, a practice that we endorse. Because the blocks of Madera Formation within the map area are fault bounded, the top and the bottom of the formation do not crop out. Exposed Madera strata probably are correlative with part of the arkose member of the Madera Formation, which was named by Lindsey (1995). His arkose member is equivalent to the arkosic limestone member of Brill (1952), and it overlies the gray limestone member that forms the basal Madera. Fossils provide age control for the Madera Formation. Ames (1957) described Desmoinesian age crinoids, brachiopods, bryozoans, pelecypods, gastropods, and fusulinids in the Madera Formation in McCarty Park about 19 miles north of the map area. Mid-Desmoinesian fusulinids were collected from the middle and upper parts of the gray limestone member in this same general area (Lindsey, 1995). Tischler (1961, 1963) assigned an Atokan age to the basal part of the Madera Formation at La Veta Pass. Estimated thickness of the incomplete section of Madera strata in the map area is about 2,000 ft.

LOWER PALEOZOIC OR NEOPROTEROZOIC INTRUSIVE ROCKS

PzZg Gabbro—A dark-greenish-gray to greenish-brown nonfoliated gabbro dike strikes northwest through foliated Paleoproterozoic gneissic granite (unit Xgg) on the west side of Lookout Mountain. A much smaller, northeast-striking gabbro dike is located just west of the Ricardo Creek fault near the southernmost exposure of gneissic granite. The larger dike is up to 150 ft wide and at least 5,800 ft long. Both dikes are vertical to steeply dipping. Gabbro is equigranular and medium grained in the interior of the dike and fine grained along margins. The gabbro often appears "salt-and-pepper" mottled on fresh surfaces. Gabbro weathers dark brown or greenish brown and forms subdued outcrops and small saddles.

The larger gabbro dike is dominated by plagioclase (labradorite) and augite, with modal abundances of 40 to 50 percent and 25 to 35 percent, respectively. The minerals grow in a subophitic manner in which plagioclase laths are partially enclosed within augite oikocrysts. This gabbro contains as much as 6 percent quartz in a micrographic texture with plagioclase, and up to 8 percent biotite. Opaque grains (likely titanomagnetite) typically average 4 to 5 percent, but range up to 12 percent. Other minerals observed in thin section include chlorite, prehnite, clay minerals, and iron oxides/hydroxides. The larger dike is locally altered; one sample consists chiefly of chlorite, prehnite, and clay minerals with only remnant plagioclase and augite visible. The smaller gabbro dike consists of hornblende (50 to 55 percent), plagioclase (25 percent), augite (5 to 8 percent), calcite (8 to 10 percent), biotite (3 percent), and opaque minerals (1 percent). The presence of calcite and sulfide minerals indicates that the small dike is probably altered. Hornblende may be a replacement after pyroxene. A few very coarse-grained "pods" of hornblende and pyroxene were noted in outcrop. Opaque minerals in the small dike include

chalcopyrite, pyrite, and sphalerite. Small amounts of olivine, iddingsite, and chlorite also are present. Five whole-rock samples of unit **PzZg** were chemically analyzed for major elements (Appendix 1).

The gabbro dikes are similar to dikes mapped north, west, and south of this map area by Lindsey (1995), Wallace and Lindsey (1996), Wallace and Soulliere (1997), Kirkham and others (2003, 2004), and Lipman and Reed (1989). The age of the dikes is not known with certainty. Nowhere in this region are these dikes known to have intruded Upper Paleozoic or younger rocks. The dikes lack evidence of the regional metamorphism that has affected the enclosing Paleoproterozoic rocks. Lipman and Reed (1989) reported a Rb-Sr age of 670 Ma for similar nonfoliated gabbro dikes along Costilla Creek in northern New Mexico. Larson and others (1985) used Rb-Sr dating on mafic dikes in the Black Canyon of the Gunnison and Unaweap Canyon, both in Colorado, to arrive at an age of 497 Ma for their emplacement. Larson and others (1985) believe that these mafic dikes were emplaced during an early Paleozoic continental rifting event.

PALEOPROTEROZOIC INTRUSIVE ROCKS

Xp Pegmatite—Pegmatite dikes intrude gneissic granite units **Xgg** and **Xag** and metamorphic units **Xa**, **Xhb**, and **Xf**. Most of the pegmatites are small lensoid and irregular masses less than 5 ft thick. Small pegmatites were not mapped individually. A few larger pegmatites 10 to 30 ft thick and up to several hundred ft long are shown on the map. Pegmatite is pink and white, very coarse grained, and non-foliated to moderately foliated. It consists predominantly of feldspar (chiefly microcline), quartz, and mica. Feldspar crystals up to 8" long were observed at a few places. In most pegmatites, the mica is biotite, but a few pegmatites that cut felsic gneiss contain muscovite rather than biotite.

Xap Aplite—Mappable masses of fine-grained, equigranular aplitic granite are present within augen gneiss (unit **Xag**) near the contact of the augen gneiss with the layered gneisses that it intruded. Only the largest masses of aplite were mapped. Most of the mapped aplite bodies are on or near Split Mountain. Narrower, discontinuous dikes of aplite are locally common within unit **Xag** and **Xgg**. Aplite is light pink to light gray and consists primarily of quartz and feldspar. Sparse biotite is present in some samples. Near the top of Split Mountain, aplite contains a few small xenoliths of felsic gneiss (unit **Xf**).

Xgg Gneissic granite—Gneissic granite is the predominant Proterozoic rock unit in the southern half of the Culebra Peak quadrangle. It crops out in the central and northern part of the map area, in the hanging wall of the Ricardo Creek fault and foot wall of the El Fragoso fault. Gneissic granite is a meta-igneous unit that intruded older layered gneisses (units **Xf**, **Xa**, and **Xhb**) that are exposed only in the northwestern part of the map area. Gneissic granite is light pinkish tan to light pinkish gray, medium grained, and equigranular. It usually weathers into angular fragments, and weathered rock surfaces are light tan to light orangish brown. Strong to moderate gneissic foliation is defined by thin, wispy, parallel bands of biotite. Foliation becomes less intense and flattened lenticular augen become discernible as gneissic granite grades into augen gneiss (unit **Xag**). Small dikes and pods of pegmatite and aplite are locally common within gneissic granite.

In thin section the gneissic granite is composed of 30 to 45 percent quartz, 25 to 40 percent microcline, 15 to 30 percent plagioclase (oligoclase), and 1 to 8 percent biotite. Accessory magnetite, zircon, and titanite (sphene) also were noted. Limonite and chlorite are present in small amounts as alteration products. Internal strain features such as bent and discontinuous plagioclase twinning and quartz with wavy grain margins are common. At many locations, particularly near major faults, biotite has been altered in varying degrees to produce orange-brown, powdery iron oxide. Three whole-rock chemical analyses of unaltered gneissic granite indicate that it is a monzogranite (Appendix 1). Two samples of gneissic granite from the adjacent La Valley quadrangle (Kirkham and others, 2004) were dated by the U.S. Geological Survey. $^{206}\text{Pb}/^{238}\text{U}$ SHRIMP dating of zircons from gneissic granite yielded ages of 1.688 Ga and 1.689 Ga (D.P. Miggins, 2004, personal communication).

Xag Granitic augen gneiss—Granitic augen gneiss forms a broad, east-northeast-trending zone enclosed within non-augeniferous granitic gneiss (unit Xgg). The trend of the main mass of granitic augen gneiss is approximately conformable to the strike of metamorphic foliation. The granitic augen gneiss is pink-gray to light-gray, coarse-grained, weakly to moderately foliated biotite granite containing microcline augen 0.4 to 2 inches long. Foliation is best defined by planar alignment of augen and biotite. The unit weathers into broad, rounded outcrops and large rounded boulders. In thin section the augen gneiss is composed of 20 to 33 percent quartz, 30 to 60 percent microcline, 10 to 25 percent plagioclase, 5 to 15 percent biotite, and locally up to 4 percent hornblende. Opaque minerals (probably magnetite) make up 0.5 to 3 percent of the rock. Similar augen gneiss mapped elsewhere in the Culebra Range contains accessory titanite (sphene), apatite, zircon, epidote, and allanite (Lipman and Reed, 1989; Wallace and Lindsey, 1996; Kirkham and others, 2004).

The granitic augen gneiss may be a less intensely deformed variety of granitic gneiss (unit Xgg). Augen are stretched into elongated, flattened lenses with increasing metamorphic foliation near mapped contacts with unit Xgg. Three whole-rock chemical analyses of unaltered granitic augen gneiss indicate that it is a monzogranite and chemically similar to gneissic granite (Appendix 1). Small differences in whole-rock chemistry between the two rock types may be attributable to subtle mineralogical differences due to the differing degrees of metamorphism affecting each of the units. Contacts between the two units are gradational.

PALEOPROTEROZOIC LAYERED ROCKS

The oldest rocks exposed in the map area comprise a thick sequence of layered gneisses into which the Proterozoic granite intruded. Xenoliths of coherent layered gneiss observed within the Proterozoic granite suggest that these layered gneisses were deposited and already metamorphosed prior to the intrusion of the Proterozoic granite at ~1689 Ma. This layered gneiss sequence is at least 1500 ft thick in the map area and continues to the south flank of Purgatoire Peak, which is immediately north of the map area. While these rocks were lumped together as “metasediments” (Xms) on the adjacent La Valley quadrangle (Kirkham and others, 2004), the overall sequence is herein subdivided on the basis of the thicknesses, mineralogical differences, and lateral continuities of submembers. In addition, the layered gneiss sequence probably has both sedimentary and igneous origins, thus the term “metasediment” may be a genetic misnomer for this sequence of rocks. The subdivisions are hornblende-biotite gneiss and amphibolite (Xhb), amphibolite (Xa), and felsic gneiss (Xf).

Xhb Hornblende-biotite gneiss and amphibolite—This sequence of rocks contains individual layers that are 1 to 7 ft thick and vary in composition from biotite- and hornblende-bearing gneisses to amphibolite. The amphibolite layers in this unit are too thin to map separately. These rocks are very well foliated, fine to medium grained, and weather dark gray to very dark grayish black. They form subdued outcrops. Unlike the amphibolite unit (Xa), these rocks do not commonly show a mesoscopic S2 fabric. Petrographically, these rocks are dominated by plagioclase, have subequal amounts of biotite, hornblende, and quartz, and contain lesser sphene and opaque grains. Given the heterogeneity of this map unit, it is believed that the protolith was a mixed volcanic/volcaniclastic unit. The thickness of the unit is indeterminate since the northern contact is an unknown distance off the map area. A similar rock package has been described by Wallace and Soulliere (1996), Wallace and Lindsey (1996), and Lipman and Reed (1989).

Xa Amphibolite—A relatively thick (100 to 200 ft) amphibolite unit crops out along the northwest margin of the map area and can be correlated across several cirques southwest of Purgatoire Peak. The amphibolite is very dark greenish gray to black on fresh surfaces, forms cliffy outcrops up to 100 ft tall, weathers dark green to dark brown, and contains millimeter-scale layers composed of dark-green hornblende, white plagioclase, and quartz. The contacts of unit Xa with underlying felsic gneisses (unit Xf) and overlying hornblende-biotite gneiss (unit Xhb) are sharp. Metamorphic foliation (S1) in the amphibolite is commonly folded, thereby yielding an S2 fabric. In places, the folding of S1 is tight enough to be considered crenulated. In addition to the development of S2 fabric, centimeter-scale quartz boudinage is present. Petrographically, the rock is dominated by hornblende with lesser quartz, plagioclase, chlorite, and epidote. The whole-rock composition of the amphibolite is listed in Appendix 1 (sample JK140). The observed homogeneity and chemistry of the amphibolite suggests the protolith was a basalt flow.

Xf Felsic gneiss—This package of quartz-rich and often muscovite- and/or biotite-bearing rocks represents the dominant unit within the suite of layered gneisses in the map area. These gneisses are fine to medium grained and are generally light gray to light brown in outcrop. On fresh surfaces the quartz and muscovite in these rocks sparkle brightly in the sunlight. Foliation is generally well developed in these gneisses, though like unit Xhb, no mesoscopic S2 fabric was

observed. In places, these gneisses contain thin layers of amphibolite. Petrographically, felsic gneisses are generally quartz-dominant (up to 50 percent) with lesser potassium feldspar and plagioclase. Quartz, potassium feldspar, and plagioclase also can occur in subequal amounts (25 to 30 percent each). In addition, muscovite, biotite, chlorite after biotite, and opaque grains are observed in thin section. In one sample the muscovite content is approximately 30 percent, which could indicate a sedimentary protolith. Similar rock units have been described in the Culebra Range by Wallace and Soulliere (1996), Wallace and Lindsey (1996), Kirkham and others (2004), and Lipman and Reed (1989).

STRATIGRAPHY

The oldest rocks in the south half of the Culebra Peak quadrangle are Paleoproterozoic igneous and metamorphic rocks that crop out on the northeast and upthrown side of El Fragoso fault in the central, north-central, and northwest parts of the map area. The crystalline Proterozoic rocks consist predominantly of a large pluton of gneissic granite (units Xgg and Xag) that extends north and west far beyond the map area. The gneissic granite is variably foliated, having been affected by post-emplacement metamorphism and shearing. Wallace and Lindsey (1996) and Wallace and Soulliere (1996) interpreted similar leucocratic granitic gneiss and augen gneiss in the Trinchera Peak and Ojito Peak quadrangles as part of a monzogranite batholith. Two samples of gneissic granite from the adjoining La Valley quadrangle (Kirkham and others, 2004) were submitted to the U.S. Geological Survey for age determination. Preliminary $^{206}\text{Pb}/^{238}\text{U}$ SHRIMP ages of 1,688 Ma and 1,689 Ma were obtained from zircons in the samples (D.P. Miggins, written commun., 2004).

Small lenticular bodies of pegmatite (unit Xp) are common throughout the gneissic granite units. Most of these bodies, which probably are dikes, are too small to show on the map. Aplite dikes (unit Xap) are fairly common within the gneissic granite units; they also typically are too small to depict on the map. A few larger aplite bodies are present on and near Split Mountain. Pegmatite and Aplite bodies probably formed during or shortly after emplacement of the granite intrusion.

The gneissic granite batholith intruded an older sequence of layered mafic and felsic gneisses (units Xhb, Xa, and Xf). These gneisses, which probably have both sedimentary and volcanic protoliths (Wallace and Soulliere, 1996), now form a northeast-striking, northwest-dipping roof pendant exposed only in the northwestern corner of the map area. A few xenoliths of these layered gneisses were found within gneissic granite near their contact.

A northwest-trending gabbro dike (unit PzZg) intrudes Paleoproterozoic gneissic granite on the west side of "Lookout Mountain" in the central part of the map area. A shorter and narrower gabbro dike is located north of the junction of Ricardo and Little Vermejo Creeks, near the Ricardo Creek fault. The gabbro dikes are similar in mode of occurrence and composition to dikes tentatively assigned a Neoproterozoic or Early Paleozoic age to the north and west (Lindsey, 1995; Wallace and Lindsey, 1996; Wallace and Soulliere, 1997; Kirkham and others, 2003, 2004). The age of the dikes is not known with certainty. However, they intrude well-foliated Paleoproterozoic rocks in this map area and show no evidence of the regional metamorphism that has affected the enclosing Paleoproterozoic rocks. Nowhere have the gabbro dikes been shown to intrude Paleozoic or younger rocks. Lipman and Reed (1989) reported a Rb-Sr age of 670 Ma for similar nonfoliated gabbro dikes along Costilla Creek in northern New Mexico. The presence of an early Paleozoic rift in the region (Larson and others, 1985) supports

this age assignment. Until absolute ages are available for the mafic intrusions in the quadrangle, it is reasonable to assume they are Neoproterozoic or early Paleozoic.

The oldest Phanerozoic sedimentary formation in the map area is the Middle Pennsylvanian Madera(?) Formation (unit **IPm**), which is mostly marine arkosic sandstone and conglomeratic sandstone, siltstone, shale, and very minor limestone. Only a partial section of the Madera Formation is preserved in the map area; faults bound both the top and bottom of this unit, and the Madera strata are entirely cut out by faulting near the southern edge of the map area. The Whiskey Creek Limestone Member of Brill (1952) was not recognized within the map area, nor was it feasible to split out other members of the Madera, as was done to the north in the Trinchera Peak quadrangle (Wallace and Lindsey, 1996). Most, and perhaps all, Madera strata within the map area are correlative with the arkose member of Wallace and Lindsey (1996), which is equivalent to the arkosic limestone member of Brill (1952). However, these strata also could be part of the lower Sangre de Cristo Formation (C.J. Fridrich, 2005, written commun.).

A thick sequence of fluvial redbeds in the Lower Permian and Upper Pennsylvanian Sangre de Cristo Formation (unit **PPsc**) comprise the youngest Paleozoic rocks in the map area. The sediments of the Sangre de Cristo Formation were eroded off the Uncompahgre-San Luis highland and deposited chiefly in alluvial fan environments in the central Colorado trough (Mallory, 1972). The basal part of the Sangre de Cristo Formation is cut out by faulting; more of the basal strata are missing in the southern part of the area than in the north.

A sequence of Triassic to Cretaceous rocks disconformably overlies the Sangre de Cristo Formation. The Triassic strata (unit **Tjt**) are very poorly exposed within the map area but are well exposed to the northeast along Johnson Creek and to the south along Ricardo Creek. The following description summarizes published studies of the good nearby exposures.

Johnson and Baltz (1960) included all the Triassic strata for at least 8 miles north of the Colorado-New Mexico boundary in the Johnson Gap Formation, a practice that was followed by Baltz (1965), Johnson (1969), and Lucas and others (1987). Pillmore (1976) assigned these Triassic rocks to the Chinle Formation and noted that the upper and middle parts of his Chinle were correlative to the Johnson Gap Formation of Johnson (1969).

Lucas and others (1990) reclassified these rocks as part of their regional study of Triassic strata in the Sangre de Cristo Mountains of New Mexico. They correlated the lower 58 ft of the 90-ft-thick section of Triassic rocks exposed along Johnson Creek (units 1-9 of Johnson and Baltz, 1960) with the Trujillo Formation. Light-gray fine-grained sandstone, greenish-gray and gray intraformational pebble conglomerates, brown claystone, and greenish-gray shale constitute the Trujillo Formation at Johnson Gap. The name Johnson Gap Formation was retained only for the upper 32 ft of Triassic strata at Johnson Gap (units 10 and 11 of Johnson and Baltz). Reddish-brown very fine- to fine-grained sandstone forms the lower two-thirds of this interval, and the upper one-third is covered.

To the south along Ricardo Creek, Lucas and others (1990) described a measured section in the Triassic rocks. Here, the Johnson Gap Formation consists of about 50 ft of grayish-green and grayish-red-purple, very fine- to medium-grained sandstone, grayish-green intraformational pebble conglomerate, and grayish-purple and light-olive-gray siltstone and mudstone. The Trujillo Formation is 39 ft thick along Ricardo Creek and consists of grayish-green very fine-grained sandstone and grayish-green intraformational conglomerate. According to Lucas and others (1990), the Triassic Baldy Hill Formation and Santa Rosa Formation (combined thickness of 54 ft) underlie the Trujillo Formation at Ricardo Creek but are not present at Johnson Gap. It

is possible that the Baldy Hill and Santa Rosa formations extend into, but are not recognized within, the map area.

The Middle Jurassic Entrada Sandstone, which was deposited in an eolian environment, disconformably overlies the Triassic rocks, and the continental sediments of the Upper Jurassic Morrison Formation overlie the Entrada. Because exposures of the Jurassic strata are sparse and poor, the Morrison Formation and Entrada Sandstone are lumped together in a single map unit (Jme). Lower Cretaceous rocks disconformably overlie the Jurassic Morrison and Entrada strata. The Lower Cretaceous rocks include the Purgatoire Formation and disconformably overlying Dakota Sandstone (unit Kdp). They were deposited on the margin of the transgressing Cretaceous Western Interior Seaway. A major Lower Cretaceous disconformity separates the Glencairn and Lytle members of the Purgatoire Formation (Kues and Lucas, 1987). The Dakota Hogback typically is held up by the erosion-resistant Dakota Sandstone and Purgatoire Formations, but the Morrison Formation and Entrada Sandstone locally form the crest of the ridge in the map area.

A conformable sequence of marine Upper Cretaceous rocks overlies the Dakota Sandstone. In ascending order, they are the Graneros Shale, Greenhorn Limestone, Carlile Shale, Niobrara Formation, and Pierre Shale. These rocks are obscured by surficial deposits in the map area and are included in a single unit (Ku).

Oligocene volcanoclastic sediments (unit Tvc) crop out in a few roadcuts east of Devils Park and south and west of Ricardo Creek. These deposits include subrounded and rounded clasts of widely varying composition that were probably eroded from major volcanic areas situated to the south near Questa (Lipman and Reed, 1989) or to the west in the San Luis Hills or San Juan Mountains (Thompson and Machette, 1989; Lipman, 2000). These weakly lithified sediments probably are Oligocene in age. A clast from a correlative volcanoclastic deposit about 0.7 miles south of the map area yielded an $^{40}\text{Ar}/^{39}\text{Ar}$ age of 31.07 ± 0.05 Ma (table 1), and a clast from another volcanoclastic deposit about 4.5 miles south of the map area was dated at 29.53 ± 0.08 Ma (Miggins and others, 2002; Miggins, 2002). These volcanoclastic deposits underlie the Amalia Tuff (Miggins, 2002; Pillmore, 2004) and pre-date initiation of rifting.

A single mafic igneous body (unit Tim) of probable Oligocene or Miocene age appears to intrude the volcanoclastic sediments near the Ricardo Creek fault east of Devils Park. The west side of the igneous body abuts or is concealed by Quaternary diamicton, and the contact with volcanoclastic sediments on the east side of the igneous body is poorly exposed. However, the finer-grained, chilled margins of the igneous body and the stratigraphic relationships between the igneous body and volcanoclastic sediments lead us to conclude it is a dike. The volcanoclastic sediments, as well as the late Cenozoic Santa Fe Group, crop out only in the overthrust block of the Ricardo Creek fault. This relationship indicates Laramide thrust structures may have influenced middle and late Cenozoic sedimentation and tectonism within the map area, similar to that described by Kellogg (1999) in other parts of Colorado.

A granodiorite stock and an associated suite of sills (unit Tgd) intruded the Upper Pennsylvanian Sangre de Cristo Formation in the northeast part of the map area. Fine-grained glassy phases are locally present along the margin of the stock, and at least one of the sills is glassy, which suggests the depth of emplacement of these intrusive rocks was relatively shallow. Esser (2005) reported a minimum cooling age of 15.23 ± 0.05 Ma for the granodiorite on the basis of $^{40}\text{Ar}/^{39}\text{Ar}$ analyses of biotite and hornblende from the granodiorite. The age spectra from these analyses, although very disturbed, suggest the granodiorite probably is Miocene in age, but it may be older.

The Santa Fe Group is the youngest bedrock unit in the map area. Hayden (1869) originally named the sediments exposed in the hills near Fort Garland and San Luis the Santa Fe Marls. Siebenthal (1910) called them the Santa Fe Formation. Kottlowski (1953) raised the rank to a group status on the basis of work in southern New Mexico. Recent regional correlations by Ingersoll and others (1990) and Chapin and Cather (1994) place all rift-related sediments and volcanic rocks younger than about 28 Ma into the Santa Fe Group.

Brister and Gries (1994) divided the Santa Fe Group in the northern half of the San Luis basin into an upper formation, which includes the fluviolacustrine Plio-Pleistocene Alamosa Formation of Siebenthal (1910), and a lower formation, which includes all other rift-related sediments and volcanic rocks. This upper formation of Brister and Gries (1994) is not present in the map area. Spiegel and Baldwin (1963) favored a group ranking for the Santa Fe “that includes all the syn-rift basin fill, both volcanic and sedimentary, ranging in age from late Oligocene to Quaternary, but excluding deposits that postdate entrenchment of the Rio Grande in middle Pleistocene time”.

For this mapping project, we use the Santa Fe group status for all syn-rift basin fill, including both sedimentary deposits and volcanic rocks. All syn-rift sediment within the map area is the informal lower Santa Fe sedimentary member (unit Tsfl) of Kirkham and others (2004); their informal upper Santa Fe sedimentary member (unit Tsfu) probably is not present in the map area. Some deposits in the downdropped block in Devils Park potentially could be correlative with the basal part of the upper member, but exposures are inadequate to conclusively demonstrate this relationship. Presence of rift-related deposits of the Santa Fe Group on and east of the crest of the Culebra Range indicate the eastern margin of the Rio Grande rift was well east of the modern range crest during the Miocene.

Syn-rift sediments are very poorly exposed in the map area. A single good exposure of these rocks was found in a cut slope along the road to Leandro Lake. A total of 18 paleocurrent directions were measured on imbricated gravel clasts in the conglomeratic beds in this outcrop. Their azimuths ranged from 186 to 250° and averaged about 207° (S27°W), indicating the stream that deposited the Santa Fe Group sediments flowed towards the modern Culebra Range at an oblique angle. The clasts within the lower Santa Fe sedimentary member are lithologically similar to the Proterozoic and Paleozoic bedrock that crops out northeast of the roadcut exposure, which supports a southwest-flowing stream direction. The crest of the Culebra Range must have been east of the easternmost extent of the Santa Fe sedimentary rocks when they were deposited, and it migrated west during the late Miocene and Pliocene. Wallace (2004) described evidence of similar relationships in the northern part of the modern Culebra Range.

Elsewhere in the map area, the lower Santa Fe Group sedimentary rocks crop out in only small, sparse, poor exposures; float mapping was an important field technique used to map and interpret these deposits. The base of the lower Santa Fe sedimentary member, which crops out in the northwest part of the map area, is rich in clasts derived from Paleozoic redbed sedimentary rocks. The proportion of redbed clasts decreases and the percentage of Proterozoic clasts increases in overlying strata. Similar relationships were noted in the La Valley quadrangle, where they were interpreted as representing an unroofing sequence (Kirkham and others, 2004).

Twenty-two samples collected from volcanic flows in the Santa Fe Group were analyzed for whole-rock major element geochemistry (Appendix 1). Rock names were assigned to each sample using the total alkali-silica diagram shown in figure 3. As in other areas on the west side of the Culebra Range (Wallace, 1996, 1997b; Wallace and Soulliere, 1996; Kirkham and others, 2003, 2004), these intercalated volcanic rocks provide much of the age control for the Santa Fe

Group. Several $^{40}\text{Ar}/^{39}\text{Ar}$ ages were obtained for volcanic flows in units Tbt and Td within and immediately adjacent to the map area during previous investigations, and two additional $^{40}\text{Ar}/^{39}\text{Ar}$ dates were obtained on these rocks during our investigation (Table 1). The geochemical data, geochronologic data, and petrologic and field relationships were utilized to define four informal volcanic map units.

One unit of basaltic to trachyandesitic rocks (unit Tbt) occurs in the map area. These rocks underlie the crest of the Culebra Range south of El Frago fault, and they also crop out in a downdropped block to the east in Devils Park. They also are widespread in the La Valley quadrangle (Kirkham and others, 2004) and can be traced as far west as the Sangre de Cristo fault, where the unit attains a thickness of about 2,000 ft. In contrast, these rocks are only 200 to 500 ft thick in the map area. Unit Tbt ranges in age from about 10.7 to 15.1 Ma, on the basis of ten $^{40}\text{Ar}/^{39}\text{Ar}$ dates on samples from within or near the map area (Table 1).

The cinder deposits of unit Tbt are well exposed in spectacular cliffs on the southeast side of the Top of the World (fig. 3). They are less well exposed in a drainage on the north side of the Top of the World. Unit Tbt consists of as much as about 600 ft of interlayered cinder beds and sparse thin lava flows. Some cinder beds contain volcanic bombs. The configuration of preserved cinder beds on the southeast side of the Top of the World (fig. 5) suggests the eruptive center for these deposits was to the east, or the cinder deposits were tilted west prior to eruption of the overlying flows unit Td. Samples from the flows and bombs are fairly heterogeneous in chemistry. They plot in basaltic trachyandesite, trachybasalt, and basaltic andesite fields (fig. 3). Miggins (2002) and Miggins and others (2002) dated three samples from the cinder deposits; they ranged from 11.80 to 11.95 Ma (Table 1). The age, chemistry, and observed stratigraphic relationships suggest the cinder deposits are in part age-equivalent to the basaltic to trachyandesitic rocks of unit Tbt.

Dacitic flows of unit Td overlie the basaltic to trachyandesitic rocks of units Tbt and Tbt at the Top of the World, which may be a constructional lava dome created by the eruption of the dacitic flows. A deposit of dacitic breccia (unit Tdb) preserved on the steep hillslope east of the Top of the World supports this conclusion. The dacitic rocks conceal and are unaffected by a fault that cuts the underlying rocks of units Tbt and Tbt. No sedimentary deposits of the Santa Fe Group overlie units Td, Tdb, or Tbt in the map area; it is possible that these volcanic rocks have been exposed at the surface since their eruption and were never covered by Santa Fe sediments. A sample of dacite (CP504A) collected during this project and analyzed by Esser (2005) using $^{40}\text{Ar}/^{39}\text{Ar}$ methods yielded an integrated or total gas age of 12.2 ± 0.1 Ma. Miggins (2002) reported an $^{40}\text{Ar}/^{39}\text{Ar}$ age of 12.08 ± 0.06 Ma for a sample collected on the west shoulder of the Top of the World that probably came from unit Td.

Quaternary surficial deposits mantle the bedrock across much of the map area. The surficial deposits include sediments of alluvial, mass-wasting, glacial, and periglacial origin, and diamicton. East of the Little Vermejo Creek fault, the surficial materials are thin, of limited areal extent, and consist entirely of alluvial and mass-wasting deposits. Surficial deposits are more widespread and a result of various origins west of the Little Vermejo Creek fault.

Glacial moraines cover much of the valley floors of Ricardo Creek, El Frago Creek, and their tributaries, extending from the cirques down the valleys to elevations as low as 9,800 ft. The sediments within the moraines, particularly the end, terminal, and ground moraines, include till, alluvium, and mass-wasting deposits; therefore these sediments are assigned to a landform-based map unit called morainal deposits. The morainal deposits are divided into two units, an older unit (Qm2), which is tentatively correlated with the Bull Lake glaciation (oxygen isotope

stage 6), and a younger unit (Qm1), which probably is correlative with the Pinedale glaciation (oxygen isotope stage 2). The younger morainal deposits locally can be subdivided into older (Qm1o) and younger (Qm1y) units on the basis of soil development and surface weathering characteristics. Deposits of glacial outwash (alluvial units Qa1, Qa2, Qa, and Qao) are found in Ricardo and El Fragoso creeks downstream of the glacial end moraines.

Extensive deposits of diamicton (units Qdi and Qdio) are found in and east of Devils Park. Although these deposits are similar to glacial till, they are not associated with distinctive cirques or nivation hollows, and their landforms are not uniquely of glacial origin. For example, a broad deposit of diamicton forms the dam for Lake Leandro. This landform vaguely resembles a subdued (old) end moraine, but it may have resulted from mass wasting. Similarly, hummocky ground with subtle, elongate ridges in the valley east of Devils Park could be ground moraine or landslide features. Without conclusive evidence of origin, we prefer to designate these deposits as diamicton.

Landslides are common within the map area. The largest landslides are along the flanks of the range crest where thick sections of weakly lithified sedimentary bedrock are overlain by a relatively thin layer of volcanic flows. Large blocks of intact but dislocated volcanic flows are locally common in these landslides. Landslides also are prevalent in Proterozoic rocks near faults and on the east side of the Dakota Hogback in the shale-rich Cretaceous units.

STRUCTURE

The south half of the Culebra Peak quadrangle straddles the structural boundary between the late Cenozoic Rio Grande rift and Laramide-age Raton basin. The San Luis basin, a major element of the Rio Grande rift extends into the quadrangle from the west, and the western margin of the Raton basin extends north-south through the eastern part of the map area.

Proterozoic rocks are widely exposed northeast of El Fragoso fault. The Paleoproterozoic rocks are part of the Southern Yavapai Province, one of a series of accreted Paleoproterozoic arc sequences that comprise the basement of the southwestern U.S. (CD-ROM Working Group, 2002; Shaw and Karlstrom, 1999). These rocks were subjected to regional metamorphism during the Paleoproterozoic that resulted in distinct foliation and folding. This regional deformation and metamorphism probably occurred during or shortly after the emplacement of voluminous Paleoproterozoic plutons (Reed and others, 1987). In the south half of the Culebra Peak quadrangle the foliation is usually parallel or subparallel to compositional layering in the gneisses, with strikes generally to the east-northeast and dips predominantly to the northwest (fig. 6). Wallace and Soulliere (1996) and Wallace and Lindsey (1996) reported that the gneissic granite and older layered gneisses were deformed into large-scale isoclinal folds with nearly parallel axes, which mainly strike ENE and E-W. Our mapping confirms the additional observation by Wallace and Lindsey (1996) that small-scale folding, boudinage, and a second set of foliations are present locally in the layered gneisses, which indicates that a later metamorphic event, possibly due to shearing, was superposed on the large-scale folds and primary foliation.

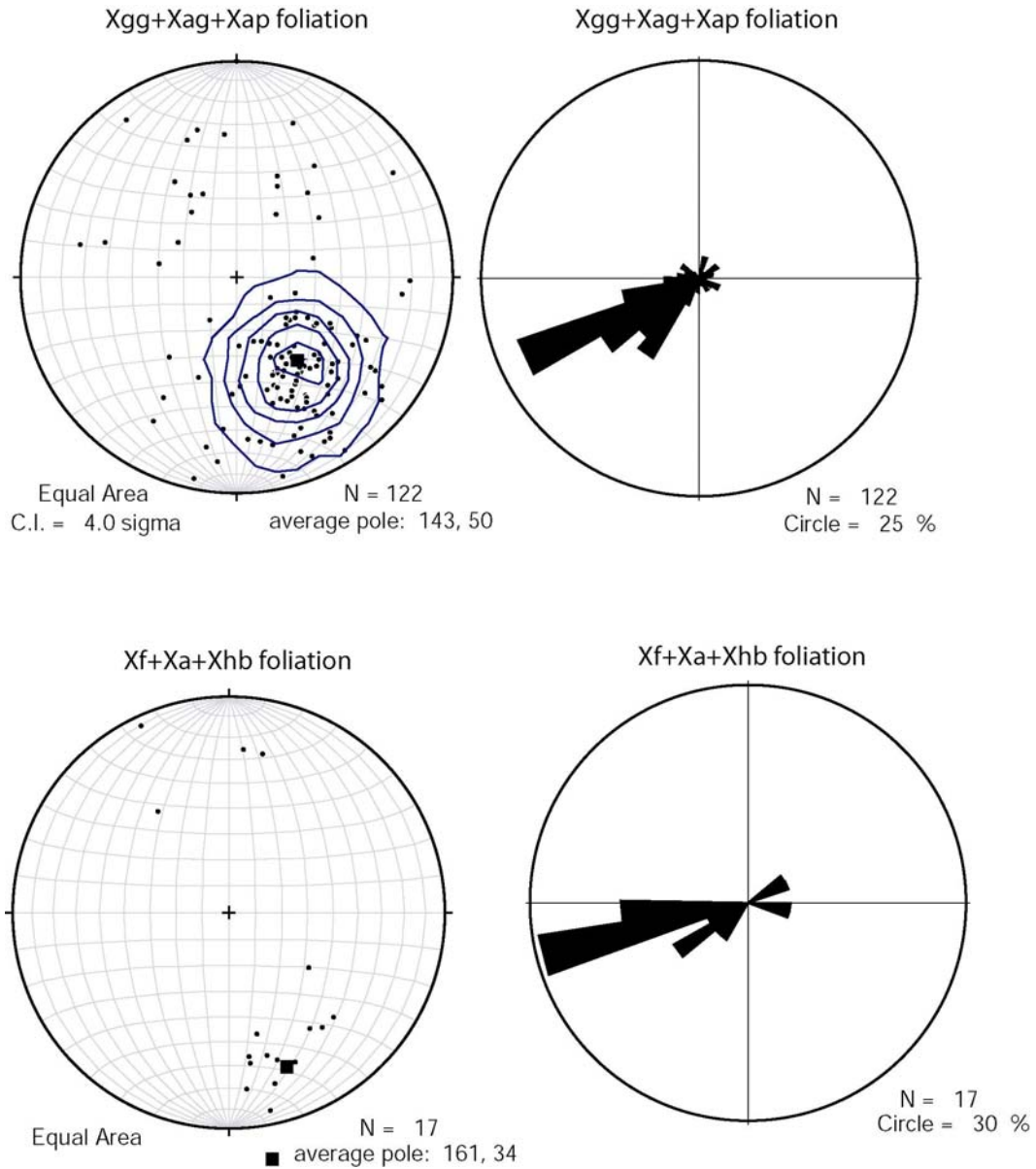


Figure 6. Stereonets and rose diagrams of foliation planes in gneissic granite (unit Xgg), granitic augen gneiss (unit Xag), aplite (Xap), felsic gneiss (unit Xf), amphibolite (unit Xa), and hornblende-biotite gneiss and amphibolite (unit Xhb) in the south half of the Culebra Peak quadrangle. Some data points shown on these graphs are not shown on the geologic map plate due to space constraints.

Numerous faults cut the Paleoproterozoic rocks in the map area. One of the more prominent faults in the Proterozoic rocks is the Split Mountain fault (fig. 7). During the late Paleozoic, sediments were eroded from the nearby uplifted Ancestral Rocky Mountains and deposited in the map area, which was part of the central Colorado trough (Mallory, 1972).

Another thick package of sediments was deposited across the south half of the Culebra Peak quadrangle when it subsided to below sea level and the Cretaceous Western Interior Seaway flooded across the region. During the late Cretaceous-early Tertiary Laramide orogeny, the western two-thirds of the map area was thrust eastward over the upper Paleozoic and Mesozoic strata. The moderately to steeply east-dipping, locally overturned upper Paleozoic and Mesozoic rocks in the footwall of the thrust form the western margin of the Raton basin.

Two major north-trending and east-verging thrust faults cross the map area. We tentatively name the western structure the Ricardo Creek fault and the eastern structure the Little Vermejo Creek fault, because relationships between these faults and previously named thrust faults to the north are ambiguous at this time. These faults form the western margin of the Raton basin within the mapped area. Proterozoic rocks overlie overturned strata of the upper Paleozoic Madera(?) Formation along the Ricardo Creek fault (fig. 8). The overturned Madera(?) strata are in turn thrust over beds of the Sangre de Cristo Formation along the Little Vermejo Creek fault. Between the Ricardo Creek and Little Vermejo Creek faults the overturned Madera(?) strata generally dip west at moderate amounts, but there are many minor faults and folds within the block that cause local dip changes (fig. 9). A few of these minor faults are approximately located on the map; many more faults probably exist.

Upper Paleozoic rocks in the footwall of the Little Vermejo Creek fault are generally overturned adjacent to the fault. To the east, these strata rapidly flatten and have southeast dips of about 35 to 50°; this structural attitude persists further east through the overlying upper Paleozoic and Mesozoic rocks. These observations lead us to conclude that most and perhaps all of the displacement on the Little Vermejo Creek fault is Laramide in age. We suspect the Ricardo Creek fault is chiefly a Laramide structure, but available data does not eliminate the possibility of late Paleozoic activity. The Ricardo Creek fault may have been re-activated in an opposite sense (down-to-west) during the Neogene, because all of the preserved Oligocene rocks and the syn-rift Santa Fe Group lie west of the fault.

Several 3-point problems were solved along the lengths of the Ricardo Creek and Little Vermejo Creek faults using points where the fault locations were well constrained by our mapping. From Round Hill to the south edge of the map area, the Ricardo Creek fault has an average strike of about N20°W and dip of 30 to 40° southwest. North of Round Hill, the dip angle of the Ricardo Creek fault is about the same, but the strike is more north-south. The strike of the Little Vermejo Creek fault is about N10°E, and most calculated dips average 40 to 50° west-northwest.

During the Oligocene, fluvial volcanoclastic sediments accumulated in a depositional basin along the southern edge of the map area, west of the Ricardo Creek fault. These same sediments may be present in the subsurface beneath Devils Park, where they would underlie the lower Santa Fe Group sediments.



Figure 7. View of Split Mountain looking north-northeast. The prominent saddle on the skyline of Split Mountain and the sharp linear valley running down the south side of the mountain mark the trace of the Split Mountain fault, which here is a relatively wide and erodable shear zone.

Near the end of the Oligocene, extensional tectonism and accompanying volcanism and sedimentation initiated in the Rio Grande rift. Miggins and others (2004) suggest rifting began at the latitude of the mapped area about 25 Ma; Brister and Gries (1994) reported a slightly earlier initiation date of 27 Ma further north in the Alamosa basin. In the southwest part of the map area, rift-related volcanic flows and sediments of the Santa Fe Group are preserved in a downdropped block on the southwest side of El Fragoso fault, a major southwest-dipping normal fault with at least 2,500 ft of post-middle Miocene throw. These Miocene sedimentary and volcanic rocks not only crop out along the crest of the Culebra Range, but they also are present in Devils Park as far as a few miles east of the range crest. The presence of age-equivalent middle Miocene volcanic flows in both locations requires the existence of at least one generally north-trending fault with significant down-to-east displacement between Devils Park and the range crest. Exposures are very poor in this area; therefore the exact position of the fault or faults is unknown. We show a single fault on the map at the western margin of Devils Park, chiefly because the northwest-striking outcrops of unit Tbt in the downdropped block terminate at this location. Other unrecognized rift-related faults may exist east of the range crest. The structure (or structures) on the east side of the range crest is responsible for over 2,000 ft of down-to-east displacement since eruption of the 12 Ma volcanic rocks in unit Tbt (see cross section C-C').



Figure 8. Ricardo Creek fault is exposed in the cut slope of a new road about 2,000 feet southeast of the top of Round Mountain. Behind and to the left of the all-terrain vehicle is strongly fractured gneissic granite (unit Xgg) in the overthrust block near the contact with the fault. The dark-purplish and red-brown beds in the vicinity of the backpack are highly fractured and oxidized clastic beds in the Madera Formation in the footwall of the thrust. The greenish-gray material between the redbeds and granite is clay gouge near the center of the fault zone, which here is about 7 to 10 feet thick. The dip of the fault plane is slightly steeper than the hillslope. View is to southeast, subparallel to the strike of the fault. ATV is about 3 ft high.



Figure 9. Overturned clastic beds in the Madera Formation on the south side of the water gap cut by Little Vermejo Creek. View is to south. Beds dip west at 65 to 70°. Note minor fault offset of rocky ledge in center of photograph.

Several lines of evidence indicate the eastern margin of San Luis basin and the Rio Grande rift was formerly east of the modern crest of the Culebra Range. This evidence includes: (1) the above mentioned presence of late Cenozoic rift-related sedimentary and volcanic rocks on and east of the modern range crest; (2) imbricated clasts in the lower Santa Fe Group sedimentary rocks near Leandro Lake in Devils Park suggest the stream that deposited these rift-related sediments flowed southwest, towards the modern range crest; and (3) the provenance area for the lower Santa Fe Group sedimentary rocks in Devils Park was northeast of the park.

ECONOMIC GEOLOGY

As done for all geologic maps produced by the CGS, a brief evaluation of the mineral resources was conducted as part of this mapping project. There are no mines of any kind, neither active nor historic, in the southern half of the Culebra Peak quadrangle. Also, no oil or gas wells have been drilled in the map area. Minor potential for small, structurally controlled vein-type gold deposits exists in the Proterozoic rocks along the El Fragoso fault zone. Though geographically remote, deposits of glacial outwash in high mountain valleys in the northern map

area represent a potential good quality gravel resource. Some of the other formations present in the quadrangle have been mined elsewhere in the state for construction material or industrial minerals. There is little or no potential for gas or oil deposits in the quadrangle, unless the late Cretaceous and early Tertiary formations in the Raton basin that host coal and coal-bed methane resources several miles east of the map area exist in the subsurface beneath the Ricardo Creek and Little Vermejo Creek thrust faults.

Metals: Rocks within the El Fragoso fault zone were sampled for gold and other trace elements at one location (JK296). At the sample site, gneissic granite is strongly brecciated and contains secondary quartz veining and locally abundant limonite and hematite. A slightly anomalous gold value of 23 parts per billion (0.023 ppm) was obtained from the sample (Appendix 2). Though far from being "ore" grade, this sample does indicate the presence of at least some gold-mineralizing activity along the steeply dipping El Fragoso fault zone.

We tested Little Vermejo Creek for placer gold using standard panning techniques. Gravel from the creek bottom was panned at five sites in the area southeast of Round Hill. No visible traces of gold were found. The gneissic granite in this area is a short vertical distance above the Ricardo Creek thrust fault and is strongly deformed by numerous thrust-related shears and possibly younger, rift-related faults. A sample of cataclastized, iron-stained, and altered gneissic granite (sample JK034) collected in this area contained no detectable gold (<1 ppb; Appendix 2).

An unpublished reconnaissance geologic map prepared by Colorado Fuel and Iron Company (Stone, 1932) shows a small "abandoned placer mine" along the Colorado-New Mexico border about 0.3 miles south of the southern boundary of the Culebra Peak quadrangle. The site is along an unnamed stream drainage that flows north into the southwest corner of Devils Park and eventually into Ricardo Creek. This area is underlain by basin-fill sediments of the Santa Fe Group, which may have hosted the reported placer. No significant production of gold has been reported from this area in the literature, and placer diggings were not observed within the southern half of the Culebra Peak quadrangle.

The eastern flank of the southern Culebra Range was explored for metals in the late 1960s and early 1970s by Colorado Fuel and Iron Company as part of their resource evaluation of the Maxwell Grant. Geochemical and aeromagnetic maps derived from their exploration effort are stored at the Bessemer Historical Society in Pueblo (map file 62-4). Maps showing the geochemical results of the stream-sediment and soil-sampling program show no anomalies of molybdenum, copper, nickel, zinc, or uranium within our map area. A few samples returned values of 120 to 140 ppm zinc, which is about three times the background value. The highest zinc concentrations were in Little Vermejo Creek. The uranium geochemistry shows that the Proterozoic rocks are slightly enriched in uranium compared to Phanerozoic sediments. The highest uranium concentration was 149 ppm in the upper reaches of the Ricardo Creek drainage. The exploration effort apparently did not include gold, since none of the maps shows results for gold analyses.

Construction Materials and Industrial Minerals: Deposits of gravelly glacial outwash are present in several of the high valleys emanating from the Purgatoire Peak area (map units Qa1, Qa2, Qa, and Qao). The outwash gravels typically are coarse grained, dominated by cobble-sized clasts derived from hard, competent Proterozoic gneiss and granite, and are potential sources of high-quality sand and gravel. Morainal deposits (units Qm1, Qm1y, Qm1o, and Qm2) also contain potentially significant gravel resources, although they can contain high amounts of fine-grained silt and sand. The weakly lithified sedimentary beds in the Santa Fe Group (unit

Tsfl) may contain potentially significant deposits of gravel and sand as well, but these deposits include more fine-grained beds and the clasts are more weathered than the much younger glacial gravel deposits. Many of the gravel clasts in the Santa Fe Group are moderately to strongly decomposed, which makes the material less suitable as a gravel resource. Gravel clasts within the volcanoclastic deposits (unit Tvc) are slightly less decomposed than those in the Santa Fe Group and hence could be a better source of pebble- and cobble-sized gravel. Volcanic members of the Santa Fe Group (units Tbt and Td), sandstone and conglomerate beds in the Dakota Sandstone and Purgatoire Formation (unit Kdp), and Proterozoic gneisses (units Xgg, Xf, Xhb, and Xa) are potential sources of crushed rock aggregate and riprap. The cinders in unit Tbt also are a potential source of light-weight aggregate and road metal. Due to the remote location of the map area, these potential aggregate and cinder deposits probably are uneconomic now, and at least into the near future, but they may be valuable for local use.

Dakota Sandstone (unit Kdp) crops out along the hogback in the southeast part of the map area. Dakota Sandstone has been mined elsewhere in Colorado for dimension stone, silica, and clay (Argall, 1949). The nearest active mines in the Dakota Sandstone are located about 60 miles north-northeast in Pueblo County (Guilinger and Keller, 2004). Beds within the Purgatoire Formation (unit Kdp) also are potential sources of dimension stone, silica, and clay. Another potential source of dimension stone, and possibly decorative stone, is the augen-rich variety of gneissic granite (unit Xag), which is highly competent and is locally relatively free of fractures in the map area. The augen impart a distinctive texture to this rock.

The Pierre Shale (included in unit Ku) is exposed east of the Dakota Hogback in the extreme southeastern corner of the map area. Pierre Shale is a potential source of common clay and lightweight aggregate. It is currently mined at a few places along the Front Range and in Pueblo County.

Although there are pegmatites (unit Xp) in the Proterozoic terrane of the map area, these probably are too small to be economic resources. Most pegmatites are less than 10 ft thick. The pegmatites are mineralogically simple, containing a mix of quartz, feldspar, and a little biotite and/or muscovite.

GEOLOGIC HAZARDS AND ENGINEERING CONSTRAINTS

Geologic hazards and engineering constraints in the south half of the Culebra Peak quadrangle include sediment-laden flooding, debris flows, rockfall, landslides, earthquakes, problematic soils, and periglacial processes. Areas underlain by alluvial unit one (Qa₁), alluvial units one and two (Qa), alluvium and colluvium (Qac), and younger fan deposits (unit Qfy) are prone to flooding, including sediment-laden flood waters, debris flows, and mud flows.

Rockfall, rock topples, and rock slides are a hazard on and beneath cliffs of hard rock. These hazards exist where (1) volcanic flows form cliffs near the range crest; (2) where Proterozoic rocks crop out in the headwalls of cirques and in the steep slopes between Lookout Mountain and Ricardo Creek, (3) at the water gap where Little Vermejo Creek cuts through upper Paleozoic rocks, and (4) along the Dakota Hogback. Areas mapped as talus (unit Qta), protalus-talus rampart deposits (unit Qptr) and some areas mapped as colluvium (unit Qc) or alluvium and colluvium (unit Qac) are particularly prone to rockfall.

Numerous large and small landslide deposits (unit Qls) are present in the map area. They are most common where relatively thin sections of volcanic rocks overlie weakly lithified Santa Fe Group sediments or where Proterozoic crystalline rocks are very fractured, such as along the

Split Mountain and El Fragoso faults (fig. 10). Landslides that were active since August 1968 when the 16,000-scale aerial photographs were flown or which are fresh appearing on these photographs are classified as young landslide deposits (unit Qlsy). Other landslide deposits (unit Qls) may have last moved during the Pleistocene or early Holocene and may be stable under present conditions.



Figure 10. Photograph of the headscarp of a landslide in fractured aplite (unit Xap) and augen gneiss (unit Xag) along the Split Mountain fault near the northern margin of the map area. View looking north towards Purgatoire Peak, which is about 0.7 miles north of the map area. The geologist stands in a prominent swale formed at the base of the headscarp (on left) and at the top of a large rotational slump of fairly intact bedrock at the head of the landslide.

Areas where past landslides have occurred (units Qlsy and Qls) may move again. Natural events such as intense rainfall, rapid snowmelt, ground shaking during earthquakes, and changes in ground-water levels can destabilize existing landslide deposits and trigger new ones. Human activities, including excavations and earth fills on slopes and changes to the hydrologic environment from irrigation, septic systems, water impoundments, and water diversions, also can contribute to slope failure.

No evidence of late Quaternary surface rupture was noted on the faults within the south half of the Culebra quadrangle during the mapping project. The likelihood of future surface rupture on these faults and accompanying earthquakes probably is less than on faults with proven

recent surface rupture. The map area, however, is susceptible to strong ground motion that might be caused by large earthquakes along the Sangre de Cristo fault, which is on the west side of the Culebra Range (Widmann and others, 2002; Kirkham and others, 2003, 2004). Several moderate-sized earthquakes also have occurred well to the east of the map area (Kirkham and Rogers, 2000; Meremonte and others, 2002) and have caused minor damage in epicentral areas (Matthews, 2003). If larger earthquakes occur in the seismically active area to the east, they could generate sufficient ground motion to affect the map area. Strong ground shaking can damage or destroy buildings and other structures. Earthquakes can also trigger secondary effects, such as liquefaction, rockfall, and landsliding, which potentially can cause great damage.

Surficial deposits derived from shale-rich Cretaceous formations, especially the Pierre Shale in the southeast part of the map area, may have high shrink-swell potential, which can be detrimental to foundations, roads, and other structures. Heaving bedrock may also be a problem in areas underlain by beds of steeply dipping Cretaceous shale on the east side of the Dakota Hogback. Fine-grained sediments deposited in fan environments and on colluvial slopes may create conditions favorable for hydrocompaction and piping. Such sediments may be found in units Qfy, Qc, and Qac.

Areas mapped as solifluction deposits (unit Qs) may experience future periglacial activity if the climate cools. These processes include frost heave, frost wedging, and slow, viscous, downslope flowage of water-saturated surficial deposits over frozen ground, all of which can be detrimental to foundations and roads.

WATER RESOURCES

The headwaters of three major river basins, the Canadian, Arkansas, and Rio Grande Rivers, lie in the south half of the Culebra Peak quadrangle. Most of the map area is drained by Fish Creek, Little Vermejo Creek, and Ricardo Creek. These small streams flow southeastward into the Vermejo River system, which joins the Canadian River near Maxwell, New Mexico. The northeast corner of the map area is drained by north- and northeast-flowing Sierra Blanca Creek and unnamed ephemeral drainages. A short distance north or northeast of the map area, surface water in these valleys flows into Johnson Creek, which is a tributary to the Purgatoire River, and eventually end up in the Arkansas River.

Both El Fragoso Creek, in the northwest part of the map area, and the East Fork of Costilla Creek, in the southwest part, are small streams within the headwaters of the Rio Grande watershed. El Fragoso Creek flows into San Francisco Creek west of the map area. The East Fork of Costilla Creek drains the southwest part of the map area. It flows southward in the map area and merges with the West Fork of Costilla Creek near the Colorado-New Mexico line to form Costilla Creek, which later joins the Rio Grande.

Ground-water resources of the map area are poorly understood, chiefly because there are no water wells in the area. Shallow ground water likely exists in alluvial aquifers in the valleys of Little Vermejo, El Fragoso, and Ricardo Creeks, and perhaps Fish and Sierra Blanca creeks. Shallow ground water also is present beneath Devils Park, as parts of this meadow are wetlands with water at or near the ground surface.

Weakly cemented sand and gravel beds in the Santa Fe Group and volcaniclastic deposits offer high potential for yielding relatively large quantities of ground water, especially in and east of Devils Park. The sedimentary and volcanic strata in the Santa Fe Group are the primary

aquifers beneath San Luis Valley. The Dakota Sandstone is a good aquifer in many parts of Colorado (Topper and others, 2003). It, along with the underlying Purgatoire Formation, may yield ground water, but these rocks are present only in a very small area in the southeast corner of the map area. Sandstone and conglomeratic beds in the Sangre de Cristo and Madera Formation also may contain ground water, but these strata are moderately well cemented and may have low porosity and permeability. Fractures in the Sangre de Cristo Formation, Madera Formation, and Proterozoic rocks may be more important sources of ground water than the intergranular pore space. Fracture spacing and fracture permeability may be more favorable for ground-water production in and near the major fault zones.

ACKNOWLEDGMENTS

This geologic mapping project was funded jointly by the Colorado Geological Survey and U.S. Geological Survey through the STATEMAP component of the National Cooperative Geologic Mapping Program, Award number 04HQOAG0075. The State of Colorado provided funding through the Department of Natural Resources Severance Tax Operational Fund, which is derived from the production of gas, oil, and minerals.

We thank Vince Matthews (CGS) for his support and field review of the mapping. We also thank Dave Noe (CGS) for his field review and assistance in interpreting and measuring paleocurrent directions in the Santa Fe sediments and in recognizing the top and bottom of beds in the overturned Madera strata. The map and report benefited from the review comments of Chris Fridrich and Michael Machette (USGS). Ren Thompson and Dan Miggins (USGS) gave us a preliminary, but very helpful, copy of the geologic map of The Wall quadrangle by the late Charles L. Pillmore. Dan Miggins also provided unpublished $^{206}\text{Pb}/^{238}\text{U}$ SHRIMP dates on gneissic granite sampled in the adjacent La Valley quadrangle, and he discussed his thesis work in the area (Miggins, 2002) on several occasions. Our understanding of the glacial deposits and diamicton benefited from discussions with Ralph Shroba (USGS) and Rich Madole (USGS-emeritus). Janet Boyd (Rocky Mountain Steel), Jay Trask (Bessemer Historical Society), Chris Carroll (CGS), and Brenda Hannu (CGS) helped us locate, examine, and reproduce reports, maps, and correspondence in the Colorado Fuel and Iron Company Archival Collection, which are preserved by the Bessemer Historical Society in Pueblo. Jason Wilson (CGS) prepared the final digital map in GIS by modifying digital files initially developed by Premier Data Services, and Larry Scott (CGS) drafted figure 1.

Special thanks go to the owners and employees of the Hill Ranch, Cielo Vista Ranch, and Vermejo Park Ranch. They include Bobby and Dottie Hill, Mike and Brenda Powell, Ted Turner, Marv Jensen, Rich Larson, and Pat McGrew. Our field work could not have been conducted without their permission and cooperation.

REFERENCES CITED

- Argall, G.O., 1949, Industrial minerals of Colorado: Quarterly of the Colorado School of Mines, v. 44, no. 2, 477 p.
- Ames, V.E., 1957, Geology of McCarty Park and vicinity, Costilla and Huerfano Counties, Colorado: Golden, Colorado School of Mines, M.S. thesis, 122 p.
- Baltz, E.H., 1965, Stratigraphy and history of Raton Basin and notes on San Luis Basin, Colorado-New Mexico: American Association of Petroleum Geologists Bulletin, v. 49, no. 11, p. 2041-2075.
- Bolyard, D.W., 1959, Pennsylvanian and Permian stratigraphy in Sangre de Cristo Mountains between La Veta Pass and Westcliffe, Colorado: American Association of Petroleum Geologists Bulletin, v. 43, no. 8, p. 1896-1939.
- Brill, K.G., Jr., 1952, Stratigraphy in the Permo-Pennsylvanian zeugogeosyncline of Colorado and northern New Mexico: Geological Society of America Bulletin, v. 63, no. 8, p. 809-880.
- Brister, B.S., and Gries, R.R., 1994, Tertiary stratigraphy and tectonic development of the Alamosa Basin (northern San Luis Basin), Rio Grande rift, south-central Colorado, *in* Keller, G.R., and Cather, S.M., eds, Basins of the Rio Grande rift-Structure, stratigraphy, and tectonic setting: Geological Society of America Special Paper 291, p. 39-58.
- Burbank, W.S., Lovering, T.S., Goddard, E.N., and Eckel, E.B., compilers, 1935, Geologic map of Colorado: U.S. Geological Survey, scale 1:500,000.
- CD-ROM Working Group, 2002, Structure and evolution of the lithosphere beneath the Rocky Mountains-Initial results from the CD-ROM experiment: GSA Today, v. 12, no. 3, p. 4-10.
- Chapin, C.E., and Cather, S.M., 1994, Tectonic setting of the axial basins of the northern and central Rio Grande rift, *in* Keller, G.R., and Cather, S.M., eds, Basins of the Rio Grande rift-Structure, stratigraphy, and tectonic setting: Geological Society of America Special Paper 291, p. 5-25.
- Cruden, D.M., and Varnes, D.J., 1996, Landslide types and processes, *in* Turner, A.K., and Schuster, R.L., eds., Landslides—Investigation and mitigation: National Research Council, Transportation Research Board Special Report 247, p. 36-75.
- Esser, R.P., 2005, $^{40}\text{Ar}/^{39}\text{Ar}$ geochronology results from the Culebra Peak and Como quadrangles, Colorado: New Mexico Geochronological Research Laboratory, Internal Report No. NMGR-L-IR-493 and 494.
- Flint, R.F., Sanders, J.E., and Rodgers, John, 1960, Diamictite, a substitute term for symmectite: Geological Society of America Bulletin, v. 71, no.12, p. 1809.
- Folk, R.L., and Ward, W.C., 1957, Brazos River bar-A study in the significance of grain size parameters: Journal of Sedimentary Petrology, v. 27, p. 3-26.
- Fullerton, D.S., Bush, C.A., and Pennell, J.N., 2003, Map of surficial deposits and materials in the eastern and central United States (east of 102° west longitude): U.S. Geological Survey Geologic Investigations Series I-2789, scale 1:2,500,000.
- Gile, L.H., Peterson, F.F., and Grossman, R.B., 1966, Morphological and genetic sequences of carbonate accumulations in desert soils: Soil Science, v. 101, p. 347-360.
- Guilinger, J.R., and Keller, J.W., 2004, Directory of active and permitted mines in Colorado – 2002: Colorado Geological Survey Information Series 68, CD-ROM.
- Guthrie, R.L., and Witty, J.E., 1982, New designations for soil horizons and layers and the new soil survey manual: Soil Science Society of America Journal, v. 46, p. 443-444.

- Hayden, F.V., 1869, Geologic report, *in* [Third annual] preliminary field report of the United States Geological Survey of Colorado and New Mexico, conducted under the authority of Hon. J.D. Cox, Secretary of Interior: Washington, D.C., Government Printing Office [reprinted in 1873 in "First, second, and third annual reports of the United States geological survey of the Territories for the years 1867, 1868, and 1869 under the Department of Interior, p. 103-251].
- Hilgard, E.W., 1892, A report on the relations of soil to climate: U.S. Department of Agriculture, Weather Bureau Bulletin 3, 59 p.
- Hungr, O., Evans, S.G., Bovis, M.J., and Hutchinson, J.N., 2001, A review of the classification of landslides of the flow type: *Environmental & Engineering Geoscience*, v. 7, no. 3, p. 221-238.
- Ingersoll, R.V., Cavazza, W., Baldrige, W.S., and Shafiqullah, M., 1990, Cenozoic sedimentation and paleotectonics of north-central New Mexico-Implications for initiation and evolution of the Rio Grande rift: *Geological Society of America Bulletin*, v. 102, p. 1280-1296.
- Ingram, R.L., 1989, Grain-size scale used by American geologists, *in* Dutro, J.T., Jr., Dietrich, R.V., and Foose, R.M., eds., *AGI data sheets for geology in the field, laboratory, and office*: Alexandria, Va., American Geological Institute, Data Sheet 29.1.
- Jackson, J.A., ed., 1997, *Glossary of geology*, 4th ed.: Alexandria, Va., American Geological Institute, 769 p.
- Johnson, R.B., 1969, Geologic map of the Trinidad 1 x 2 degree quadrangle, south-central Colorado: U.S. Geological Survey Miscellaneous Investigations Map I-558, scale 1:250,000.
- Johnson, R.B., and Stephens, J.G., 1954, Geology of the La Veta area, Huerfano County, Colorado: U.S. Geological Survey Oil and Gas Investigations Map OM-146, scale 1:31,680.
- Johnson, R.B., and Baltz, E.H., 1960, Probable Triassic rocks along eastern front of Sangre de Cristo Mountains, south-central Colorado: *Bulletin of American Association of Petroleum Geologists*, v. 44, no. 12, p. 1895-1902.
- Keller, G.R., Cordell, L., Davis, G.H., Peeples, W.J., and White, G., 1984, A geophysical study of the San Luis Basin, *in* Baldrige, W.S., Dickerson, P.W., Riecker, R.E., and Zidek, J., eds., *Rio Grande rift-Northern New Mexico*: New Mexico Geological Society, 35th Annual Field Conference, p.51-57.
- Kellogg, K.S., 1999, Neogene basins of the northern Rio Grande rift-Partitioning and asymmetry inherited from Laramide and older uplifts: *Tectonophysics*, v. 305, p. 141-152.
- Kirkham, R.M., and Heimsoth, C.M., 2003, Geologic map of the Fort Garland SW quadrangle, Costilla County, Colorado: Colorado Geological Survey Open-File Report 02-6, scale 1:24,000.
- Kirkham, R.M., Lufkin, J.L., Lindsay, N.R., and Dickens, K.E., 2004, Geologic map of the La Valley quadrangle, Costilla County, Colorado: Colorado Geological Survey Open-File Report 04-8, scale 1:24,000.
- Kirkham, R.M., and Rogers, W.P., 2000, Colorado earthquake information, 1867-1996: Colorado Geological Survey Bulletin 52, 160 p., CD-ROM.
- Kirkham, R.M., Shaver, K.C., Lindsay, N.R., and Wallace, A.R., 2003, Geologic map of the Taylor Ranch quadrangle, Costilla County, Colorado: Colorado Geological Survey Open-File Report 03-15, scale 1:24,000.
- Kottowski, F.A., 1953, Tertiary-Quaternary sediments of the Rio Grande valley in southern New Mexico: *New Mexico Geological Society Guidebook 4*, p. 144-148.
- Kues, B.S., and Lucas, S.G., 1987, Cretaceous stratigraphy and paleontology in the Dry Cimarron Valley, New Mexico, Colorado, and Oklahoma, *in* Lucas, S.G., and Hunt, A.P., eds., *Northeastern New Mexico*: New Mexico Geological Society Guidebook 38, p. 167-198.
- La Roche, H. de, 1992, A cationic homologue of the QAP triangle (quartz-alkali feldspar-plagioclase), a major feature of plutonic rock petrology: *Comptes Rendus de l'Académie des Sciences Paris*, v. 315, Serie II. p. 1687-1693.

- Larson, E.E., Paterson, P.E., Curtis, G., Drake, R., and Mutschler, F.E., 1985, Petrologic, paleomagnetic, and structural evidence of a Paleozoic rift system in Oklahoma, New Mexico, Colorado, and Utah: *Geological Society of America Bulletin*, v. 96, p. 1364-1372.
- Le Bas, M.J., LeMaitre, R.W., Streckeisen, A.I., and Zanettin, B., 1986, A chemical classification of volcanic rocks based upon the total alkali-silica diagram: *Journal of Petrology*, v. 27, p. 747-750.
- Lindsey, D.A., 1995, Geologic map of the McCarty Park quadrangle, Costilla and Huerfano Counties, Colorado: U.S. Geological Survey Miscellaneous Field Studies Map MF-2282, scale 1:24,000.
- Lindsey, D.A., 1996, Geologic map of the Cuchara Pass quadrangle, Huerfano and Las Animas Counties, Colorado: U.S. Geological Survey Miscellaneous Field Studies Map MF-2294, scale 1:24,000.
- Lipman, P.W., 2000, Central San Juan caldera cluster-Regional volcanic framework, *in* Bethke, P.M., and Hay, R.L., eds., *Ancient Lake Creede-Its volcano-tectonic setting, history of sedimentation, and relation to mineralization in the Creede mining district*: Geological Society of America Special Paper 346, p. 9-69.
- Lipman, P.W., and Reed, J.C., Jr., 1989, Geologic map of the Latir volcanic field and adjacent areas, northern New Mexico: U.S. Geological Survey Miscellaneous Investigations Series I-1907, scale 1:48,000.
- Lucas, S.G., Hunt, A.P., and Hayden, S.N., 1987, The Triassic System in the Dry Cimarron Valley, New Mexico, Colorado, and Oklahoma, *in* Lucas, S.G., and Hunt, A.P., eds., *Northeastern New Mexico*: New Mexico Geological Society, Guidebook 38, p. 97-117.
- Lucas, S.G., Hunt, A.P., and Huber, Phillip, 1990, Triassic stratigraphy in the Sangre de Cristo Mountains, New Mexico, *in* Bauer, P.W., Lucas, S.G., Mawer, C.K., and McIntosh, W.C., eds., *Tectonic development of the southern Sangre de Cristo Mountains, New Mexico*: New Mexico Geological Society, Guidebook 41, p. 305-318.
- Machette, M.N., 1985, Calcic soils of the southwestern United States, *in* Weide, D.L., ed., *Soils and Quaternary geology of the southwestern United States*: Geological Society of America Special Paper 203, p. 1-21.
- Mallory, W.W., 1972, Regional synthesis of the Pennsylvanian System, *in* Mallory, W.W., ed., *Geologic atlas of the Rocky Mountain region*: Rocky Mountain Association of Geologists, p. 111-127.
- Matthews, V., 2003, The challenges of evaluating earthquake hazard in Colorado, *in* Boyer, D.D., Santi, P.M., and Rogers, W.P., 2003, *Engineering geology in Colorado*: Colorado Geological Survey Special Publication 55, CD ROM.
- Meremonte, M.E., Lahr, J.C., Frankel, A.D., Dewey, J.W., Crone, A.J., Overturf, D.E., Carver, D.L., and Bice, W.T., 2002, Investigation of an earthquake swarm near Trinidad, Colorado, August-October 2001: U.S. Geological Survey Open-File Report 02-0073, version 1, available online at <http://pubs.usgs.gov/of/2002/ofr-02-0073/ofr-02-0073.html>.
- Miggins, D.P., 2002, Chronologic, geochemical, and isotopic framework of igneous rocks within the Raton Basin and adjacent Rio Grande rift, south-central Colorado and northern New Mexico: Boulder, University of Colorado, M.S. thesis, 417 p.
- Miggins, D.P., Thompson, R.A., Pillmore, C.L., Snee, L.W., and Stern, C.R., 2002, Extension and uplift of the northern Rio Grande rift-Evidence from $^{40}\text{Ar}/^{39}\text{Ar}$ geochronology from the Sangre de Cristo Mountains, south-central Colorado and northern New Mexico, *in* Menzies, M.A., Klemperer, S.L., Ebinger, C.J., and Baker, J., eds., *Volcanic rifted margins*: Geological Society of America Special Paper 362, p. 47-64.
- Pillmore, C.L., 1976, Supplementary road log to Ricardo Creek section, an exposure of lower Mesozoic rocks near the New Mexico-Colorado state line, *in* Ewing, R.C., and Kues, B.S., *Guidebook of Vermejo Park, northeastern New Mexico*: New Mexico Geological Society, Guidebook 27, p. 45-47.
- Pillmore, C.L., 2004, unpublished geologic map of The Wall quadrangle, New Mexico.
- Pillmore, C.L., and Eicher, D.L., 1976, Lower part of the marine Cretaceous at Gold Creek, Vermejo Park, New Mexico, *in* Ewing, R.C., and Kues, B.S., *Guidebook of Vermejo Park, northeastern New Mexico*: New Mexico Geological Society Guidebook, 27th field conference, p. 171-176.

- Reed, J.C., Jr., Bickford, M.E., Premo, W.R., Aleinikoff, J.N., and Pallister, J.S., 1987, Evolution of the Early Proterozoic Colorado province—Constraints from U-Pb geochronology: *Geology*, v. 15, no. 9, p. 861-865.
- Shaw, C.A., and Karlstrom, K.E., 1999, The Yavapai-Mazatzal crustal boundary in the southern Rocky Mountains: *Rocky Mountain Geology*, v. 34, p. 37-52.
- Siebenthal, C.E., 1910, *Geology and ground-water resources of the San Luis Valley, Colorado*: U.S. Geological Survey Water-Supply Paper 240, 128 p.
- Soil Survey Staff, 1975, *Soil taxonomy*: U.S. Department of Agriculture Handbook 436, 754 p.
- Spiegel, Z., and Baldwin, B., 1963, *Geology and water resources of the Santa Fe area, New Mexico*: U.S. Geological Survey Water-Supply Paper 1525, 258 p.
- Stone, J.B., 1932, *Geologic map of the Maxwell Grant*: unpublished map prepared for the Colorado Fuel and Iron Company, Bessemer Historical Society, Pueblo, Colorado, CF&I Archival Collection file number 280-8028-5.
- Streckeisen, A., 1976, To each plutonic rock its proper name: *Earth Science Reviews*, v. 12, p. 19-28.
- Thompson, R.A., and Machette, M.N., 1989, *Geologic map of the San Luis Hills area, Conejos and Costilla Counties, Colorado*: U.S. Geological Survey Miscellaneous Investigations Series I-1906, scale 1:50,000.
- Tischler, H., 1961, *The Pennsylvanian and Permian stratigraphy of the Huerfano Park area, Colorado*: Ann Arbor, University of Michigan, Ph.D. dissertation, 200 p.
- Tischler, H., 1963, Fossils, faunal zonation, and depositional environment of the Madera Formation, Huerfano Park, Colorado: *Journal of Paleontology*, v. 37, no. 5, p. 1054-1068.
- Topper, R., Spray, K.L., Bellis, W.H., Hamilton, J.L., and Barkmann, P.E., 2003, *Ground water atlas of Colorado*: Colorado Geological Survey Special Publication 53, 210 p.
- Tweto, O., 1978, Tectonic map of the Rio Grande rift system in Colorado, *in* Hawley, J.W., compiler, *Guidebook to Rio Grande rift in New Mexico and Colorado*: New Mexico Bureau of Mines and Mineral Resources Circular 163, scale 1:1,000,000.
- Tweto, O., 1979, compiler, *Geologic map of Colorado*: U.S. Geological Survey, scale 1:500,000.
- Vine, J.D., 1974, *Geologic map and cross sections of the La Veta Pass, La Veta, and Ritter Arroyo quadrangles, Huerfano and Costilla Counties, Colorado*: U.S. Geological Survey Miscellaneous Investigations Series I-833, scale 1:48,000.
- Waage, K.M., 1953, Refractory clay deposits of south-central Colorado: *U.S. Geological Survey Bulletin* 993, 104 p.
- Wallace, A.R., 1995, Cenozoic rift-related sedimentation and faulting, northern Culebra Range, southern Colorado, *in* Bauer, P.W., Kues, B.S., Dunbar, N.W., Karlstrom, K.E., and Harrison, Bruce, eds., *Geology of the Santa Fe region: New Mexico Geological Society Guidebook, 46th Field Conference*, p. 147-154.
- Wallace, A.R., 1996, *Geologic map of the Trinchera Ranch quadrangle, Costilla County, Colorado*: U.S. Geological Survey Miscellaneous Field Studies Map MF-2312-C, scale 1:24,000.
- Wallace, A.R., 1997a, *Geologic map of the Fort Garland quadrangle, Costilla County, Colorado*: U.S. Geological Survey Miscellaneous Field Studies Map MF-2312-E, scale 1:24,000.
- Wallace, A.R., 1997b, *Geologic map of the Russell quadrangle, Costilla County, Colorado*: U.S. Geological Survey Miscellaneous Field Studies Map MF-2312-D, scale 1:24,000.
- Wallace, A.R., 2004, Evolution of the southeastern San Luis basin margin and the Culebra embayment, Rio Grande rift, southern Colorado, *in* Brister, B.S., Bauer, P.W., Read, A.S., and Leuth, V.W., eds., *Geology of Taos region: New Mexico Geological Society 2004 Field Trip Guidebook*, p. 181-192.
- Wallace, A.R., and Lindsey, D.A., 1996, *Geologic map of the Trinchera Peak quadrangle, Costilla, Huerfano, and Las Animas Counties, Colorado*: U.S. Geological Survey Miscellaneous Field Studies Map MF-2312-A, scale 1:24,000.
- Wallace, A.R., and Soulliere, S.J., 1996, *Geologic map of the Ojito Peak quadrangle, Costilla County, Colorado*: U.S. Geological Survey Miscellaneous Field Studies Map MF-2312-B, scale 1:24,000.

- Widmann, B.L., Bartos, P.J., Madole, R.F., Barba, K.E., and Moll, M.E., 2004, Geologic map of the Alma quadrangle, Park and Summit Counties, Colorado: Colorado Geological Survey Open-File Report 04-3, scale 1:24,000.
- Widmann, B. L., Kirkham, R. M., Morgan, M. L., and Rogers, W. P., with contributions by Crone, A. J., Personius, S. F., and Kelson, K. I.; GIS and Web design by Morgan, K. S., Pattyn, G. R., and Phillips, R. C., 2002, Colorado late Cenozoic fault and fold database and internet map server: Colorado Geological Survey Information Series 60a, web publication available at <http://geosurvey.state.co.us/pubs/ceno>.

APPENDIX 1

Whole-Rock Major-Element Geochemical Analyses [All analyses were performed by ALS Chemex using the XRF method. Refer to the map for sample locations and explanation of map unit symbols.]

Sample no.	Unit	SiO ₂	Al ₂ O ₃	Fe ₂ O ₃	CaO	MgO	Na ₂ O	K ₂ O	Cr ₂ O ₃	TiO ₂	MnO	P ₂ O ₅	SrO	BaO	LOI	Total
		(in Weight %)														
CP1	Tbt	53.21	16.20	7.67	6.95	3.25	4.64	2.51	0.01	1.43	0.07	0.65	0.16	0.17	2.12	99.04
CP2	Tbt	52.47	14.54	8.72	7.27	6.04	3.97	2.27	0.02	1.54	0.11	0.67	0.18	0.16	1.22	99.20
CP29	Tim	53.56	15.13	7.63	5.75	5.67	3.41	2.68	0.01	1.17	0.10	0.45	0.10	0.16	3.79	99.62
CP37A	Tgd	65.31	15.15	3.25	2.70	1.05	4.44	3.24	<0.01	0.45	0.04	0.28	0.06	0.15	3.04	99.17
CP46	Tgd	66.94	15.69	3.86	2.87	1.17	3.84	3.35	<0.01	0.52	0.04	0.17	0.06	0.14	1.20	99.82
CP62	Tbt	46.27	14.94	11.53	8.54	5.19	2.73	1.68	0.02	1.85	0.14	0.71	0.14	0.12	5.89	99.77
CP69	Tbt	45.27	14.65	11.50	9.00	7.85	3.70	1.27	0.03	1.93	0.15	0.79	0.22	0.12	2.40	98.88
CP82	Tbt	46.11	14.50	11.17	9.64	6.88	3.27	1.54	0.02	1.84	0.15	0.73	0.19	0.12	3.49	99.65
CP106	Tbt	53.52	14.65	8.21	7.03	5.54	4.06	2.39	0.02	1.35	0.11	0.67	0.18	0.15	0.38	98.25
CP120	Tbt	50.26	14.48	8.70	8.30	4.90	3.77	2.46	0.02	1.57	0.11	0.81	0.19	0.17	2.93	98.66
CP123	Tbt	52.40	14.10	7.40	9.13	4.11	3.80	2.55	0.02	1.25	0.10	0.70	0.17	0.17	3.43	99.33
CP249	Tgd	67.20	15.31	3.66	2.74	1.06	3.81	3.29	0.01	0.49	0.05	0.14	0.06	0.13	1.54	99.50
CP266	Td	63.24	16.19	4.25	3.76	1.57	4.72	2.82	<0.01	0.64	0.05	0.26	0.10	0.13	0.35	98.08
CP269	Tbt	47.41	13.60	9.72	10.30	5.24	3.51	2.13	0.03	1.98	0.13	0.65	0.15	0.12	4.71	99.68
CP271	Tdb	65.75	15.42	4.15	3.67	1.88	4.64	2.61	<0.01	0.61	0.05	0.24	0.10	0.12	0.55	99.80
CP271A	Tbt	50.33	13.78	10.10	8.09	6.23	3.64	2.14	0.02	1.98	0.13	0.81	0.18	0.16	2.05	99.63
CP299	Tbt	51.02	14.10	10.02	7.50	6.65	3.84	2.17	0.03	2.12	0.13	0.65	0.16	0.14	1.09	99.61
CP503	Tbt	49.10	14.70	8.40	9.00	5.40	4.00	2.43	0.02	1.50	0.12	0.78	0.19	0.17	3.26	99.08
CP504A	Td	63.59	16.62	4.62	3.80	1.63	4.71	2.85	<0.01	0.70	0.06	0.29	0.10	0.13	0.39	99.50
CP504B	Td	63.43	16.74	4.56	3.86	1.62	4.70	2.87	<0.01	0.70	0.06	0.30	0.10	0.13	0.38	99.45
CP508	Tbt	50.70	14.88	8.80	7.35	6.37	3.58	2.39	0.03	1.55	0.11	0.80	0.18	0.16	2.83	99.73
CP600	Td	64.28	16.79	4.22	3.55	1.42	4.85	2.77	<0.01	0.66	0.06	0.29	0.12	0.13	0.60	99.73
CP604	Tbt	53.10	14.98	8.55	7.26	6.25	3.76	2.29	0.02	1.43	0.12	0.71	0.18	0.16	0.89	99.70
CP605	Tbt	51.05	14.32	8.46	7.91	6.24	3.73	2.41	0.02	1.50	0.11	0.80	0.19	0.15	2.90	99.81
JK014	PzZg	48.77	15.91	12.97	6.30	4.10	3.01	1.80	0.01	2.42	0.18	0.58	0.04	0.05	2.27	98.41
JK022	Xgg	75.25	12.65	1.88	0.39	0.12	2.88	4.80	0.01	0.20	0.02	0.02	<0.01	0.04	0.56	98.82
JK078	Xag	69.05	14.11	3.97	1.37	0.44	2.75	5.15	0.01	0.52	0.07	0.08	0.01	0.10	0.56	98.19
JK132	Xag	71.08	13.31	3.52	1.38	0.45	2.65	5.07	0.01	0.46	0.06	0.06	0.01	0.09	0.41	98.56
JK140	Xa	49.25	16.10	11.42	10.16	6.21	2.59	0.58	0.02	0.65	0.23	0.15	0.05	0.03	0.93	98.37
JK159	PzZg	53.06	15.49	10.02	5.98	4.32	3.79	1.94	0.02	1.62	0.16	0.32	0.03	0.06	2.46	99.26
JK189	Xgg	73.25	13.59	1.84	0.70	0.14	3.16	5.09	0.01	0.23	0.03	0.02	0.01	0.03	0.41	98.51
JK216	PzZg	46.45	15.02	12.24	9.65	5.70	3.00	0.78	0.03	2.08	0.16	0.34	0.02	0.02	3.54	99.02
JK227	Xgg	73.55	12.89	2.59	0.71	0.27	2.62	5.33	0.01	0.31	0.05	0.05	0.01	0.06	0.52	98.98
JK245	PzZg	41.98	10.49	11.13	13.12	9.20	3.70	0.66	0.05	0.74	0.25	0.33	0.08	0.01	6.60	98.34
JK288	Tbt	48.67	13.86	9.65	7.79	7.03	2.57	1.12	0.03	1.86	0.12	0.76	0.16	0.13	5.54	99.29
JP059	Xag	68.66	14.26	3.99	1.11	1.02	2.92	5.02	0.01	0.56	0.05	0.09	0.02	0.13	0.96	98.80
JP127	PzZg	47.95	14.83	12.70	9.30	6.76	2.06	0.78	0.03	1.95	0.19	0.27	0.04	0.03	1.82	98.72
JP245	Tbt	44.56	13.40	6.52	14.03	3.35	3.46	2.47	0.01	1.23	0.09	0.75	0.19	0.14	8.37	98.56

APPENDIX 2

Trace-Element Geochemical Analyses [All analyses were performed by ALS Chemex using the ICP-MS method. Refer to the map for sample locations and map unit symbols. (ppm = parts per million)]

Sample no.	Unit	Au	Ag	Al	As	Ba	Be	Bi	Ca	Cd	Ce	Co	Cr
		ppm	ppm	%	ppm	ppm	ppm	ppm	%	ppm	ppm	ppm	ppm
JK034	Xgg sheared	<0.001	<0.01	6.19	1.40	370	3.76	0.16	0.06	<0.02	108	1.30	76.00
JK296	Xgg breccia	0.023	<0.01	6.32	0.70	810	1.72	0.23	0.04	0.03	129	4.90	73.00
		Cs	Cu	Fe	Ga	Ge	Hf	In	K	La	Li	Mg	Mn
		ppm	ppm	%	ppm	ppm	ppm	ppm	%	ppm	ppm	%	ppm
JK034	Xgg sheared	3.74	24.40	1.24	19.35	0.12	1.0	0.084	3.81	28.2	30.4	0.06	60
JK296	Xgg breccia	2.19	5.20	3.03	20.70	0.24	1.7	0.117	4.97	57.2	34.6	0.05	461
		Mo	Na	Nb	Ni	P	Pb	Rb	Re	S	Sb	Se	Sn
		ppm	%	ppm	ppm	ppm	ppm	ppm	ppm	%	ppm	ppm	ppm
JK034	Xgg sheared	4.99	0.08	25.8	3.5	110	21.0	204	<0.002	0.01	0.10	<1	7.9
JK296	Xgg breccia	0.89	0.08	15.5	5.1	280	20.5	156	<0.002	<0.01	2.15	1	4.5
		Sr	Ta	Te	Th	Ti	Tl	U	V	W	Y	Zn	Zr
		ppm	ppm	ppm	ppm	%	ppm	ppm	ppm	ppm	ppm	ppm	ppm
JK034	Xgg sheared	18.5	2.01	<0.05	37.0	0.130	0.87	1.8	9	4.2	32.1	31	23.7
JK296	Xgg breccia	101	1.04	<0.05	17.5	0.116	0.87	7.8	12	3.6	20.1	43	50.6